Miscellaneous Paper W-95-2
September 1995

US Army Corps of Engineers
Waterways Experiment Station

Water Quality Research Program

Methane Sampling Technique and the Measurement of Plunge Pool Impact on Gas Transfer Rates at Low-Head Hydraulic Structures

by David E. Hibbs, John S. Gulliver,
University of Minnesota

John P. McDonald,
Zenk Read Trygstad and Associates, Inc.

Approved For Public Release; Distribution Is Unlimited

Prepared for Headquarters, U.S. Army Corps of Engineers

The contents of this report are not to be used for advertising, publication, or promotional purposes. Citation of trade names does not constitute an official endorsement or approval of the use of such commercial products.

PRINTED ON RECYCLED PAPER

Water Quality
Research Program

Miscellaneous Paper W-95-2
September 1995

Methane Sampling Technique and the Measurement of Plunge Pool Impact on Gas Transfer Rates at Low-Head Hydraulic Structures

by David E. Hibbs, John S. Gulliver

St. Anthony Falls Hydraulic Laboratory
Department of Civil and Mineral Engineering
University of Minnesota
Minneapolis, MN 55455

John P. McDonald

Zenk Read Trygstad and Associates, Inc.
Albert Lea, MN 56007

Final report

Approved for public release; distribution is unlimited

Prepared for U.S. Army Corps of Engineers
Washington, DC 20314-1000

Monitored by U.S. Army Engineer Waterways Experiment Station
3909 Halls Ferry Road, Vicksburg, MS 39180-6199

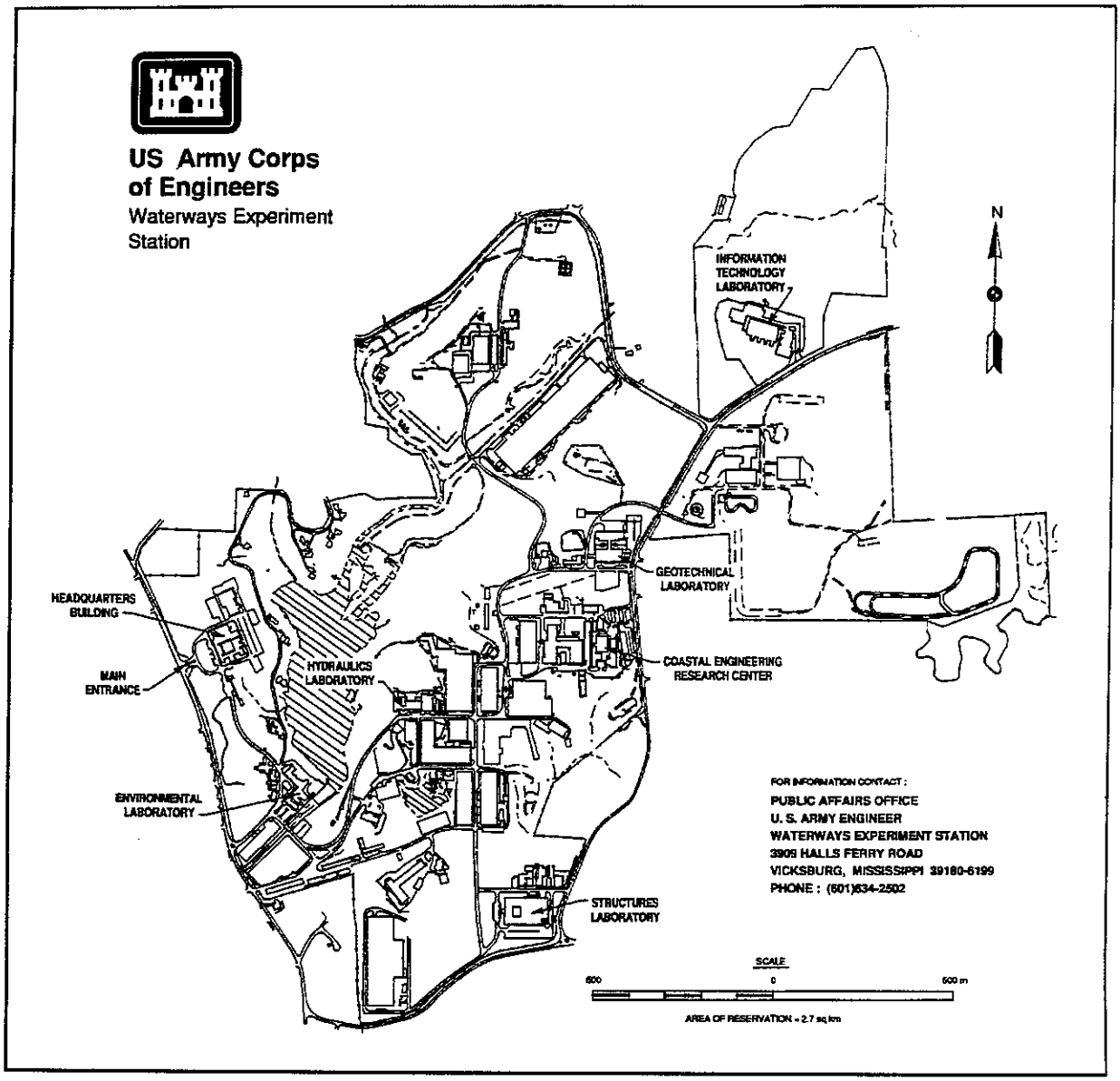

Waterways Experiment Station Cataloging-in-Publication Data

Hibbs, David E.
Methane sampling technique and the measurement of plunge pool impact on gas transfer rates at low-head hydraulic structures / by David E. Hibbs, John S. Gulliver, John P. McDonald ; prepared for U.S. Army Corps of Engineers ; monitored by U.S. Army Engineer Waterways Experiment Station.
69 p. : ill. ; 28 cm. — (Miscellaneous paper ; W-95-2)
Includes bibliographic references.
1. Methane — Sampling. 2. Hydraulic structures. 3. Rivers — Aeration. I. Gulliver, John S. II. McDonald, John P. III. United States. Army. Corps of Engineers. IV. U.S. Army Engineer Waterways Experiment Station. V. Water Quality Research Program. V. Title. VI. Series: Miscellaneous paper (U.S. Army Engineer Waterways Experiment Station) ; W-95-2.
TA7 W34m no.W-95-2

Contents

Preface vi

Conversion Factors, Non-SI to SI Units of Measurement viii

1—Introduction 1

2—Methane in the Water Column 3

Process of Methane Production 3
Methane Concentrations 5

3—Theory and Analysis 8

Gas Transfer at Hydraulic Structures 8
Indexing Gas Transfer 9
Comparison of Oxygen and Methane Transfer Efficiencies 10
Effective Saturation Concentration and Effective Bubble Depth 13
Impact of Assuming a Zero Saturation Concentration for Methane 14

4—Sampling Technique 18

Dissolved Oxygen Sampling 18
Total Dissolved Gas Sampling 18
Methane Sampling 19
Sample preservation 21
Sample transporting 22
Alternative sample shipping technique 22

5—Headspace Analysis Technique 28

Calculation of Methane Concentration in Water 28
Creating the Headspace 29
Gas Chromatography 29
Injection technique 30
Limit of detection/limit of quantification 31
Bubble Formation 33

6—Results 34

7—Conclusions 42

References 44

Photos 1-3

Appendix A: Air Entrainment Data A1
Appendix B: Description of Structures B1
Appendix C: Notation C1
SF 298

List of Figures

Figure 1. Methane isopleth from Coon Rapids Dam, 01 August 1989 . . . 6
Figure 2. Methane isopleth from Coon Rapids Dam, 06 October 1989 . . . 7
Figure 3. Oxygen transfer efficiency versus methane transfer efficiency indexed to oxygen 11
Figure 4. Air entrainment at plunge pool surface 12
Figure 5. Total gas meter calibration 20
Figure 6. Effect of formalin on methane concentration 21
Figure 7. Potential evasion routes of methane during sample transport 25
Figure 8. Restricted flow of gas from sample immersed in water bath 26
Figure 9. GC Calibration 30
Figure 10. Impact of injection speed on GC response 31
Figure 11. Effective depth versus specific discharge at Rum River Dam 38
Figure 12. Effective depth versus specific discharge at St. Cloud Dam 39
Figure B1. Plan view of Kost Dam B2
Figure B2. Profile view of Kost Dam B3
Figure B3. Plan view of Rum River Dam B4
Figure B4. Profile of Rum River fixed weir B5
Figure B5. Profile of Rum River tainter gate B6
Figure B6. Plan view of St. Cloud Dam B7
Figure B7. Profile view of St. Cloud Dam B8
Figure B8. Profile view of Smithland Lock and Dam B9
Figure B9. Profile view of Opekiska Lock and Dam B10

List of Tables

Table 1. Methane Concentrations, Opekiska Lock and Dam, September 24, 1992 23

Table 2. Methane Concentrations, Smithland Lock and Dam, September 23, 1992 24

Table 3. Data Used for LOQ Analysis 32

Table 4. Results of Simultaneous Methane and Oxygen Transfer Measurements at Various Hydraulic Structures 35

Table 5. Results of Simultaneous Methane, Oxygen, and Nitrogen Transfer Measurements at Rum River Dam, August 31, 1993 41

Preface

The work reported herein was conducted as part of the Water Quality Research Program (WQRP), Work Unit 32369. The WQRP program is sponsored by the Headquarters, U.S. Army Corps of Engineers (HQUSACE), and is assigned to the U.S. Army Engineer Waterways Experiment Station (WES) under the purview of the Environmental Laboratory (EL). Funding was provided under Department of the Army Appropriation No. 96X3121, General Investigation. The WQRP is managed under the Environmental Resources Research and Assistance Programs (ERRAP), Mr. J. L. Decell, Manager. Mr. Robert C. Gunkel, Jr., was Assistant Manager, ERRAP, for the WQRP. Technical Monitors during this study were Mr. Friedrick B. Juhle, Mr. Rixie Hardy, and Dr. John Bushman, HQUSACE.

This report details an investigation into the development of in situ methane as a tracer for oxygen uptake in plunge pools at low-head hydraulic structures. The research was conducted by the St. Anthony Falls Hydraulic Laboratory (SAFHL), Department of Civil and Mineral Engineering, University of Minnesota, under contract with the Reservoir Water Quality Branch (RWQB), Hydraulics Laboratory (HL), WES. Mr. Steven C. Wilhelms, RWQB, was the WES point of contact. The work was conducted under the general direction of Messrs. Frank A. Herrmann, Jr., Director, HL, and Glenn A. Pickering, Chief, Hydraulic Structures Division, HL. Dr. John W. Keeley was Director, EL.

Funding for the research was provided by the RWQB, WES, and by the Minnesota State Legislature, ML 1989, Chap. 335, Sec. 29, Subd. 82, as recommended by the Legislative Commission on Minnesota Resources. Thanks to Mr. Wilhelms for allowing us to use his air entrainment data and for general discussions on the topic. Thanks also to Professor Michael J. Semmens for the availability of the gas chromatograph and to Mr. John R. Thene for advice on developing the headspace technique for methane.

This report was prepared by Mr. David E. Hibbs and Dr. John S. Gulliver, SAFHL, and Mr. John P. McDonald, Zenk, Read, Trygstad, and Associates, Inc., Albert Lea, MN.

At the time of publication of this report, Director of WES was Dr. Robert W. Whalin. COL Bruce K. Howard, EN, was Commander of WES. Dr. Roger L. A. Arndt was Director, SAFHL.

This report should be cited as follows:

Hibbs, D. E., Gulliver, J. S., and McDonald, J. P. (1995). "Methane sampling technique and the measurement of plunge pool impact on gas transfer rates at low-head hydraulic structures," Miscellaneous Paper W-95-2, U.S. Army Engineer Waterways Experiment Station, Vicksburg, MS.

The contents of this report are not to be used for advertising, publication, or promotional purposes. Citation of trade names does not constitute an official endorsement or approval of the use of such commercial products.

Conversion Factors, Non-SI to SI Units of Measurement

Non-SI units of measurement used in this report can be converted to SI units as follows:

Multiply	By	To Obtain
cubic feet	0.02831685	cubic meters
feet	0.3048	meters
gallons (U.S. liquid)	3.785412	liters
inches	2.54	centimeters

1 Introduction

Hydraulic structures have a large impact on the amount of dissolved gases in a river system. Even though the water passes over the structure for only a short time, the water flowing over a spillway or weir entrains air bubbles, creating significantly more air-water surface area for gas transfer. In addition, the high turbulence that occurs at most hydraulic structures will increase the transfer rate coefficients. The same quantity of gas transfer that normally would occur in several miles in a river can occur at a hydraulic structure.

The transfer of oxygen from the atmosphere to the water is often of interest; therefore, it seems logical to directly measure oxygen transfer. However, there are some problems associated with the measurement of dissolved oxygen (DO) concentration. If the DO level is close to saturation (within approximately 2.5 mg/ℓ), the tremendous uncertainty associated with the current measurement techniques makes the estimation of gas transfer useless (Gulliver and Wilhelms 1992). Also, if the reservoir is stratified, it is difficult to predict withdrawal from the various layers with the required precision, and usually impossible to sample at the spillway crest (Gulliver and Rindels 1993). Because the required field conditions for accurate DO measurement often do not occur, other measurement techniques, such as the tracer technique, are used.

The first tracer technique for reaeration rate measurement in open channels was introduced by Tsivoglou (1968). The basic assumption behind Tsivoglou's technique is that the ratio between the desorption of the tracer gas and the absorption rate of oxygen is a constant. The ratio of tracer gas transfer rate to the oxygen transfer rate can be determined through laboratory experiments involving the simultaneous transfer of both gases. Since the driving force of gas transfer is the partial pressure difference between the concentration in equilibrium with the atmosphere, which is linearly proportional to the partial pressure in the atmosphere and that dissolved in water, tracers that have no significant atmospheric component should be chosen. Thus, measurements can be made with a tracer saturation concentration of essentially zero. Tsivoglou injected radioactive krypton-85 into a river and measured its desorption along the river reach. Tsivoglou's technique worked rather well but required the use of radioactive materials.

Rathbun et al. (1978) modified Tsivoglou's method by substituting propane and ethylene in place of krypton-85 to avoid the use of radioactive materials. The assumptions made were similar to Tsivoglou's with changes made for the desorption rates of propane and ethylene. One major restriction is that measurable quantities of the tracer could only be obtained by bubbling the gas through pneumatic diffusers, requiring additional field equipment. A more extensive review of gas tracer techniques is given in McCutcheon (1989).

Thene and Gulliver (1990) developed a headspace measurement technique for propane gas tracer and subsequently found measurable amounts of naturally occurring methane in the samples. The unanticipated quantities of methane held promise for the use of methane as a tracer gas. Methane is produced in the sediments as a by-product of the anaerobic decomposition of organic materials. No injection of artificial tracer gases is needed, which can be a substantial savings in cost and effort at the larger hydraulic structures. In addition, the uncertainty associated with the transverse mixing of the injected tracers is eliminated. The technique is more effective at low-head structures since stratification of methane has been observed at higher head structures (Wilhelms et al. 1993).

McDonald and Gulliver (1992) measured oxygen and methane transfer over several hydraulic structures. After correction for diffusivities, oxygen and methane transfer efficiencies were found to be comparable at a given structure except when the entrained air bubbles were pulled to a depth in the tail water. Because of the high static and dynamic pressures that a bubble experiences in a plunging jet flow, the concentration of atmospheric gases will be greater in the bubble than at the water surface. The rate of gas transfer will correspondingly be higher for oxygen and nitrogen due to the higher saturation concentration of the water in contact with the bubble. This problem was delineated by determining an "effective" saturation concentration from oxygen and methane measurements that incorporates the higher pressure exerted on bubbles in the plunge pool.

This report describes the development and testing of the methane tracer technique for determining gas transfer rates at low-head hydraulic structures. The effect of the plunge pool on the gas transfer rate is also examined by comparing the tracer gas transfer rate with the rate for oxygen and nitrogen.

2 Methane in the Water Column

Process of Methane Production

Methane is produced as a by-product of the anaerobic decomposition of organic material. Methanogenesis is the terminal process in a chain of decomposition processes in the anaerobic hypolimnion and represents a major mechanism by which carbon leaves the sediments (Strayer and Tiedje 1978). Methane transfer out of the sediments and hypolimnia is by vertical diffusion and, if enough methane is produced, by bubble ebullition.

Methane production is a two-stage process. In the first stage, a group of faculative and obligate bacteria, termed acid formers, turn proteins, carbohydrates, and fats into fatty acids by hydrolysis and fermentation. Methane-producing bacteria then convert these acids into methane. Some alcohols from carbohydrate fermentation can also be converted to methane by methane-producing bacteria (Wetzel 1975).

The concentration of acetate, H_2, and CO_2, the major substrates for methane production, is highly variable and is dependent upon the organic material. Acetate is the preferred substrate for methanogenesis at low partial pressures of H_2. As the partial pressure of hydrogen rises, bicarbonate is the preferred substrate.

The reaction of methane production from the reduction of carbon dioxide is given as:

$$CO_2 + 8H^+ \rightarrow CH_4 + 2H_2O \tag{1}$$

In the second process, the production of methane from acetic acid can be shown as:

$$CH_3COOH \rightarrow CH_4 + CO_2 \tag{2}$$

The later process is thought to produce about 70 percent of methane in the water column with much of the remainder coming from the reduction of CO_2. Fermentation of other acids are of less importance.

Bacteria that produce methane are strictly anaerobic. Even slight traces of oxygen are toxic to these bacteria. They consist of four major genre: rod-shaped, nonsporiferous Methanobacterium, rod-shaped sporiferous Methanobacillus, the spherical Methanococcus, and Methanosurcina. These bacteria have a wide temperature range for growth. Zeikus and Winfrey (1976) found methanogenesis occurring at temperatures from 4 to 45 °C, although the rates were highly temperature dependent. A change of 12 °C in the temperature of the sediments during the change of seasons was associated with a 100- to 400-fold increase in the rate of methanogenesis.

Methanogenesis is severely limited by sulfate reduction. Waters that have high methane concentration generally have low sulfate concentrations and vice versa. This is because the sulfate-reducing bacteria successfully compete with the methane-producing bacteria for H_2 and acetate, both precursors of methane production (Abram and Nedwell 1978). The reduction of sulfate in the sediments is described by

$$SO_4^- + 9H^+ \rightarrow HS^- + 4H_2O \tag{3}$$

Millimolar quantities of sulfate will inhibit methane production. The sulfate-reducing bacteria have a higher affinity for hydrogen and acetate than methane-producing bacteria, thus keeping the pool of these substrates at a level too low to be used by the methane-producing bacteria (Lovley et al. 1982). In addition, thermodynamic calculations can be used to predict the exclusion of methane production in sulfate containing sediments.

Very little of the methane produced in lakes or reservoirs escapes to the atmosphere because of the relatively quiescent nature of the water body or the low turbulence intensities near the water surface. Rudd (1979) measured evasion rates of 5 percent of the total methane produced. Fallon et al. (1980) measured an evasion rate of 9 percent in Lake Mendota, Wisconsin. The small evasion rates are due to the presence of methane-oxidizing bacteria, with aerobic methane oxidation that is given by:

$$5CH_4 + 8O_2 \rightarrow 2(CH_4) + 3CO_2 + 8H_2O \tag{4}$$

Because the residence time over a hydraulic structure is short, it is assumed that no significant methane oxidation occurs over the time it takes a methane molecule to pass through a structure. For example, while the half-life of methane over a structure is on the order of seconds due to the large surface area and high turbulence of the flow, the half-life of methane in the river and reservoir is on the order of hours. Therefore, it is assumed that the only pathway

for a methane molecule to leave the water column during the retention time over a structure is by evasion to bubbles or the atmosphere.

Methane Concentrations

Methane was sampled in a number of reservoirs to estimate how often one could expect relatively high (above the limit of quantification, LOQ) methane concentrations. Methane concentrations were sampled in seven reservoirs during fall, winter, and spring; in all but one reservoir, they were well above the current LOQ of 0.3 µg/ℓ (the LOQ is developed in Chapter 6). Sample methane isopleths obtained from the Coon Rapids Dam are shown in Figures 1 and 2. The concentrations varied from 119 to 4 µg/ℓ in the six reservoirs. All six reservoirs were fairly shallow, with depths ranging from 3 m (10 ft) to 9 m (30 ft). The exception was one relatively deep (18-m or 60-ft) reservoir with a methane concentration of approximately 0.5 µg/ℓ. This reservoir was held back by a hollow gravity dam, and the leakage into the hollow center had a strong hydrogen sulfide smell. As mentioned previously, methanogenesis is severely limited by sulfate production, which is believed to be occurring in this reservoir.

Methane was supersaturated at all locations sampled. This agrees with results from de Angelis and Lilley (1987). The bacterial oxidation of methane and methane evasion rates (i.e., the pathways by which methane escapes from the water column) are inadequate to remove all the methane from these reservoirs.

Methane concentrations were also not highly stratified in the shallow reservoirs except under ice cover, where methane was found at many sites at much larger concentrations just under the ice than near the sediments. This may be due to methane bubbles rising from the sediments. The ice cover would block methane evasion to the atmosphere, leaving the water just under the ice at a higher concentration. Another thought is that perhaps the ice itself contains a high amount of methane, and the water in contact with the melting ice in early spring will also have a correspondingly high methane concentration. Methane stratification may also be due to inputs into the river/reservoir.

Results of these field measurements show that under conditions of thermal stratification in reservoirs, methane will also be stratified, although not as strongly as oxygen. The highly active photic zone near the reservoir surface will enhance the naturally occurring oxygen stratification. Such is not the case for methane. The primary service that methane can provide as a gas tracer, however, would be as a substitute for O_2 and N_2 transfer at structures associated with nonstratified reservoirs, when the two gases are close to saturation. Methane will likely be present at measurable quantities and will be well above saturation.

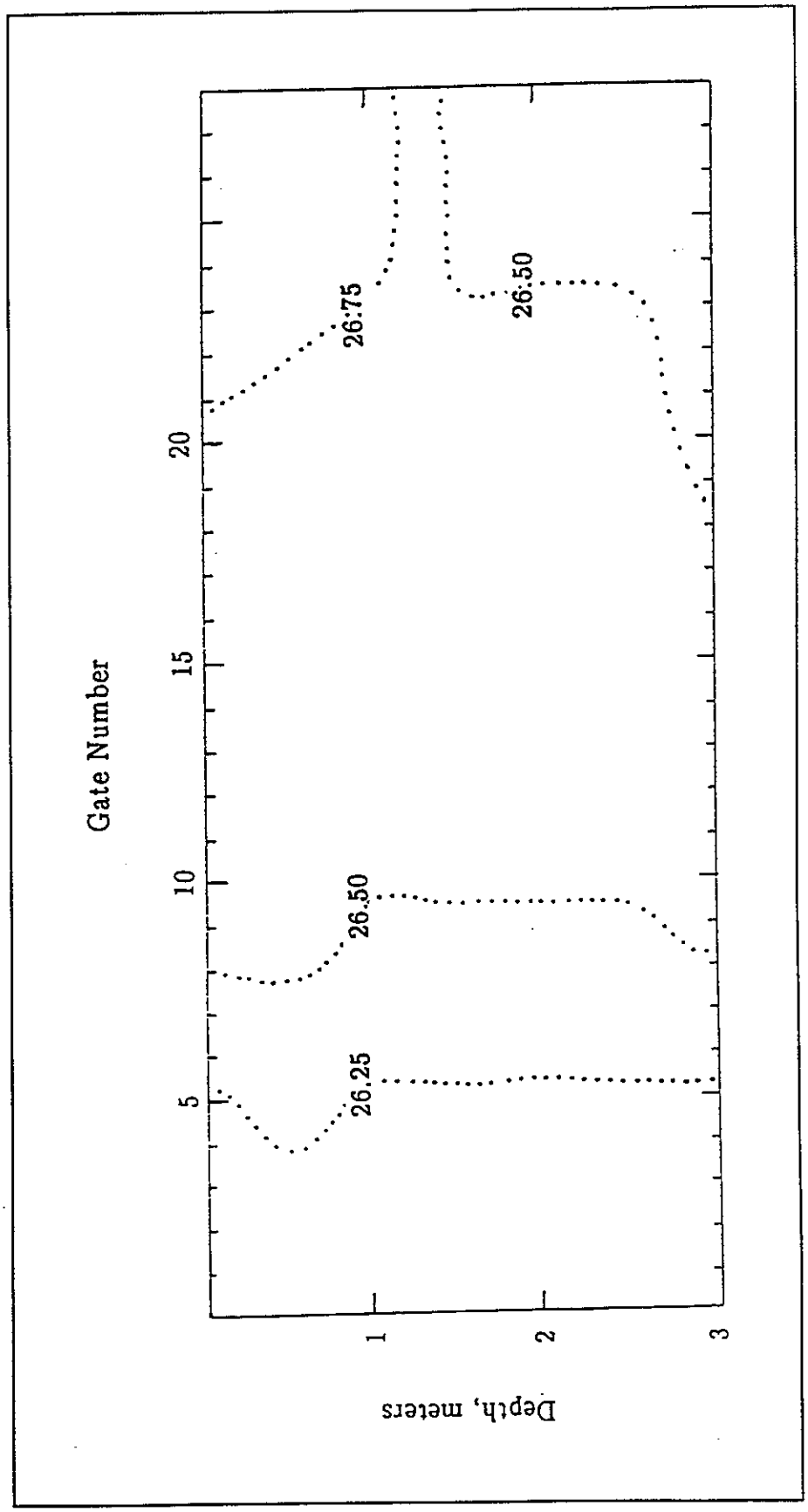

Figure 1. Methane isopleth from Coon Rapids Dam, 01 August 1989

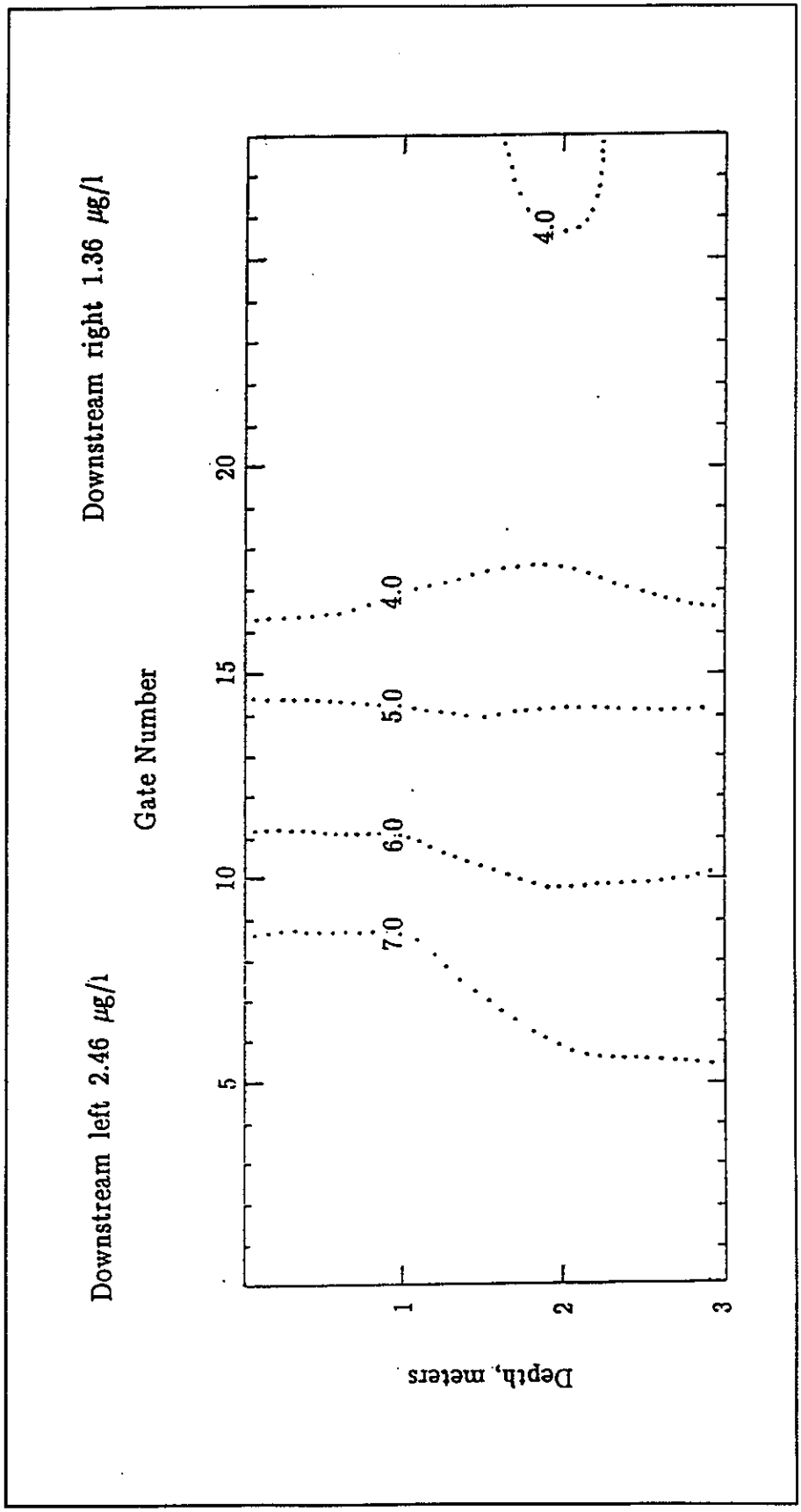

Figure 2. Methane isopleth from Coon Rapids Dam, 06 October 1989

3 Theory and Analysis

Gas Transfer at Hydraulic Structures

Gas transfer is typically described as a first-order process in which the rate of change of the gas concentration in the water is linearly dependent on the concentration difference or driving force. The flux of any volatile dissolved chemical across an air-water interface may be given by the equation:

$$F = \frac{V}{A}\frac{dC}{dt} = K_L\left(\frac{C_a}{H} - C\right) \tag{5}$$

where

F = mass flux rate per unit surface area

V = Control volume over which C and A are measured

A = Air-water interface surface area

C = Concentration of dissolved chemical in water

t = Time

K_L = Liquid film coefficient

C_a = Concentration of chemical in air

H = Henry's law constant, an equilibrium partitioning constant

C_a/H is often called the saturation concentration, C_s. Because the chemicals oxygen, nitrogen, and gas tracers of interest are volatile, only the liquid phase resistance to transfer (K_L) is considered. The gas phase resistance is much less than the liquid phase resistance, and is therefore neglected.

For transfer at a hydraulic structure, Equation 5 can be integrated from upstream of the structure to downstream of the structure, resulting in an equation for transfer efficiency (Gulliver and Rindels 1993):

$$E = \frac{C_d - C_u}{C_s - C_u} = 1 - \exp\left[-\int_{t_u}^{t_d} K_L \frac{A}{V} dt\right] \tag{6}$$

where the subscripts "*u*" and "*d*" refer to measurement locations upstream and downstream of the structure, respectively. A transfer efficiency of 1.0 means the full gas transfer up to the saturation value has occurred. No gas transfer would correspond to E = 0.0. A transfer efficiency of greater than 1.0 means the gas has become supersaturated downstream. For gases that do not have appreciable concentrations in the atmosphere (like methane), C_a and C_s are close to zero, and transfer efficiency can be written as:

$$E = \frac{C_u - C_d}{C_u} \quad \textit{(nonatmospheric gas transfer)} \tag{7}$$

Indexing Gas Transfer

Gulliver et al. (1990) developed an indexing relationship to directly compare liquid phase controlled transfer efficiencies, such as those considered herein, at hydraulic structures. This relationship can be used to index transfer measurements to a common temperature and a common gas (most often oxygen is used in gas transfer measurements). The relationship is given as:

$$E_{iO} = 1 - (1 - E_m)^{1/f_i} \tag{8}$$

where E_m is the measured transfer efficiency, i.e., the transfer efficiency of methane, and E_{iO} is the equivalent transfer efficiency of the index gas , i.e., oxygen, at the index temperature. The parameter f_i is given as

$$f_i = f_g f_T \tag{9}$$

where f_g is the diffusivity correction and f_T is the temperature correction, approximated by a curve fit to the original equation as:

$$f_T = 1.0 + 0.02103(T-20) + 8.261\times10^{-5}(T-20)^2 \tag{10}$$

where T is the temperature in °C. If the methane transfer measurements are made at the index temperature, no temperature indexing is needed and f_t is set

equal to 1. The parameter f_g may be determined from the parametric relationship given by Hanratty (1991) and Rathbun (1990) to be:

$$f_g = \left[\frac{D}{D_o}\right]^{1/2} \tag{11}$$

where D is the diffusivity of the measured compound, methane, and D_o is the diffusivity of oxygen. Rathbun (1990) and Gulliver et al. (1990) give techniques to estimate D for various compounds. The diffusivity of methane in water was researched by Thene and Gulliver (1990), who searched *Chemical Abstracts* from 1965 through 1986 and found 14 measured diffusivities with a mean value of 1.69×10^{-9} m^2/sec at 20 °C. The diffusivity of oxygen (2.18×10^{-9} m^2/sec) and Equation 11 were then used to compute an f_g value of 0.88 for the indexing of methane transfer measurements to oxygen and vice versa.

Comparison of Oxygen and Methane Transfer Efficiencies

Simultaneous oxygen and methane measurements allow for the comparison of their transfer efficiencies. Figure 3 shows the measured oxygen transfer efficiencies plotted against the methane transfer efficiencies indexed to oxygen for five low-head structures. The oxygen transfer efficiency measurement was generally equal to or higher than the methane transfer efficiency, after indexing to an equivalent oxygen transfer, indicating a discrepancy between the two simultaneous measurements.

One possible cause of this discrepancy could be that the indexing between methane and oxygen transfer was incorrect. There is some debate over the power to be applied to the diffusivity ratio, which some have said should be two-thirds rather than one-half at low turbulence levels. Aside from the fact that flow at prototype hydraulic structures is highly turbulent, this difference in power would not have a significant effect on f_g. The use of an incorrect f_g could not account for the variations in inequity between indexed methane and measured oxygen transfer efficiencies given in Figure 3. It would simply bias the results to one side or the other of perfect agreement.

A more likely cause of the incongruency of the methane and oxygen transfer efficiencies is due to the effect of tail water on gas transfer. As illustrated in Figure 4, the plunging water jet at the surface will carry entrained air bubbles to some depth. The hydrostatic force of the water column will result in a greater pressure inside these entrained bubbles as the bubbles are pulled deeper. Additionally, as the jet reaches the bottom of the plunge pool, some force acts on the flow to remove the vertical component of velocity, deflecting the spillway jet horizontally out of the plunge pool. This force also increases the pressure on the entrained bubbles. The increased pressures yield a greater

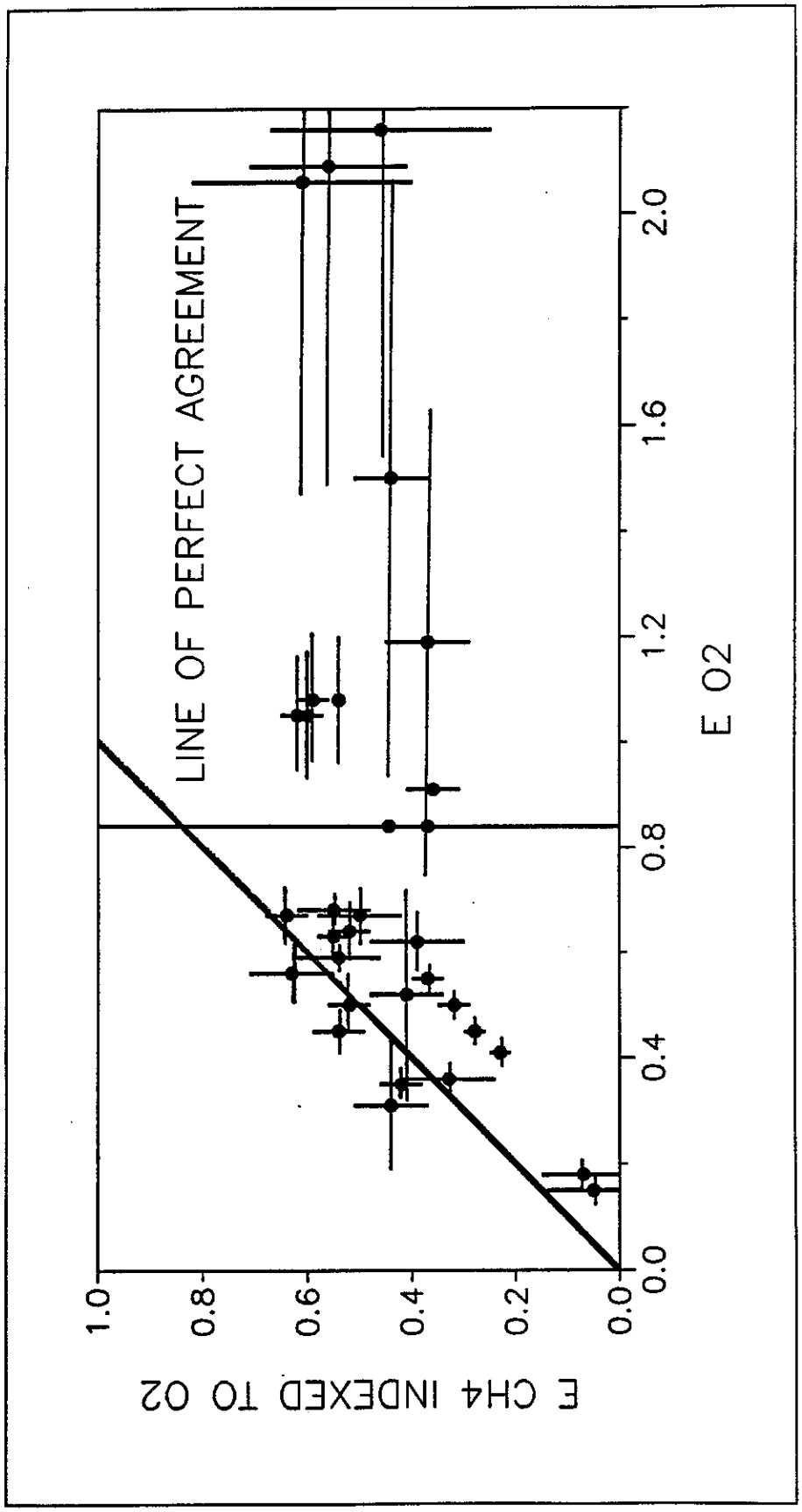

Figure 3. Oxygen transfer efficiency versus methane transfer efficiency indexed to oxygen

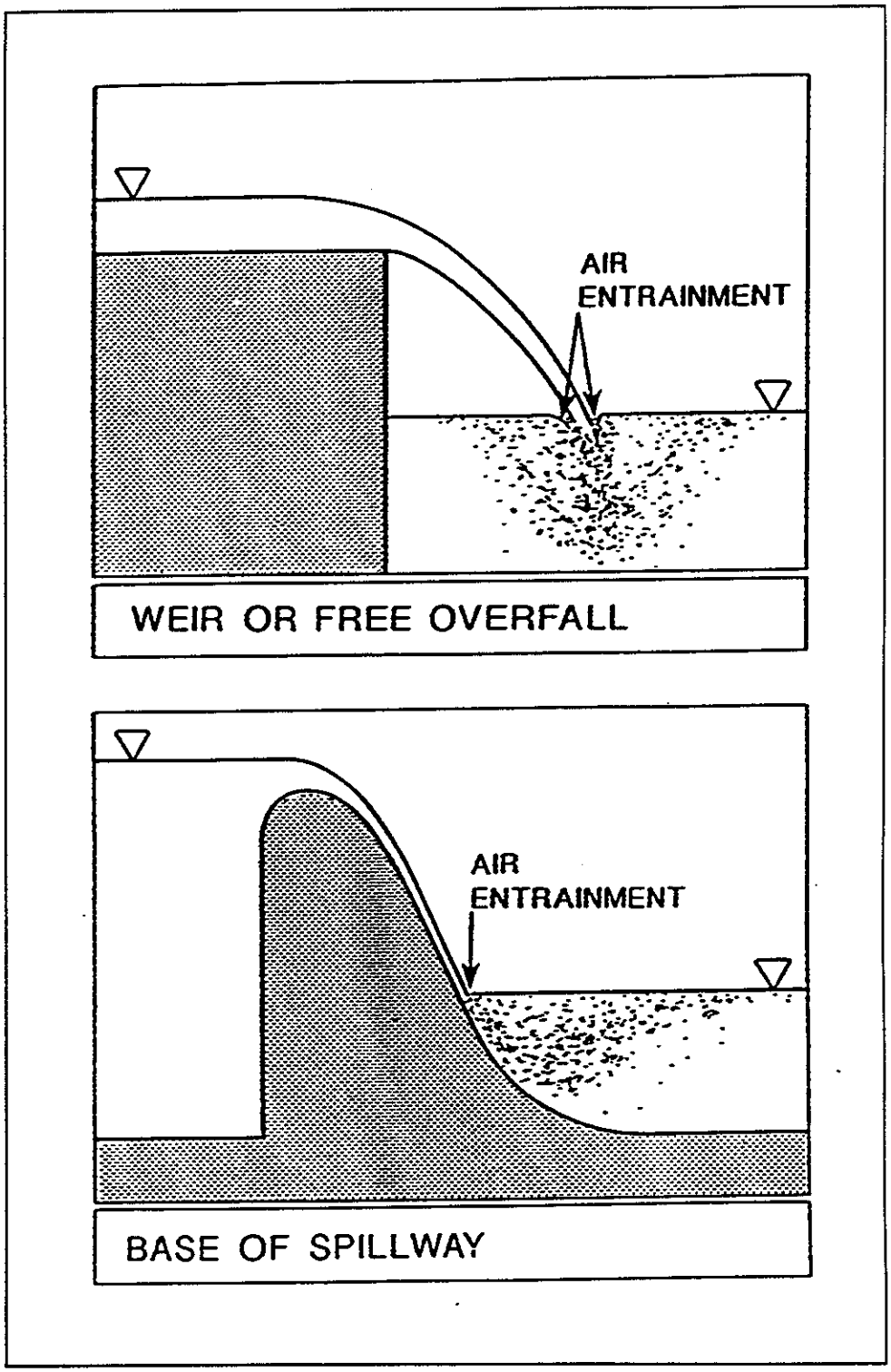

Figure 4. Air entrainment at plunge pool surface

partial pressure of oxygen in the bubbles, and hence, an increased saturation concentration than would occur at atmospheric pressure.

This phenomenon increases the transfer of atmospheric gases such as oxygen and nitrogen, since the bubbles will contain significant amounts of these gases. However, for methane and other gases that do not have significant atmospheric concentrations, the hydrostatic and dynamic forces acting in the plunge pool will not increase the gas transfer rate since the partial pressures of these gases in a bubble will be close to zero in most cases. This will be shown for one typical structure later in the report.

The integration of Equation 5 to result in Equation 6 assumed that the saturation concentration was constant. For methane transfer, the saturation concentration is essentially zero regardless of the pressure within the bubble, and therefore Equation 6 is applicable. However, for atmospheric gases, this is obviously not true. Thus, an oxygen transfer efficiency measurement should assume a saturation concentration that corresponds to pressures somewhat higher than atmospheric. Determination of this pressure and corresponding saturation concentration is one of two primary objectives of this report. The primary justification is that when a tracer, such as methane, is being used to predict an oxygen or nitrogen transfer efficiency, or when the oxygen or nitrogen transfer efficiency is being used to predict the transfer of other non-atmospheric gases, substantial errors could result. In addition, accurate prediction of oxygen and nitrogen transfer at hydraulic structures with a plunge pool is not possible without some quantification of this tail water effect (Johnson 1984). A technique is therefore needed to adjust for the higher pressure that the entrained bubbles experience in the tail water pool of a hydraulic structure.

Effective Saturation Concentration and Effective Bubble Depth

The technique used to adjust for the higher pressure that the entrained bubbles experience in the plunge pool assumes that methane and either oxygen or nitrogen concentration measurements have been made at the structure. The process is then to (a) measure the methane transfer efficiency, E_m, of the structure using Equation 7; (b) then index the methane transfer efficiency to an oxygen or nitrogen transfer efficiency with Equation 8; and (c) then use the upstream and downstream dissolved oxygen (DO) or dissolved nitrogen measurements with the indexed transfer efficiency to compute an "effective" saturation concentration for oxygen or nitrogen, C_{se}:

$$C_{se} = \left[\frac{C_d - C_u}{E_{iO}}\right] + C_u \tag{12}$$

where E_{iO} is the measured methane transfer efficiency indexed to an oxygen or nitrogen transfer efficiency and C_u and C_d are the measured DO or dissolved nitrogen concentrations upstream and downstream, respectively.

The effective saturation concentration is therefore a mean of the oxygen or nitrogen saturation concentrations that the bubbles experience, weighted by their impact on gas transfer. This weighted mean saturation concentration is not determined by following bubble paths through a plunge pool, but is simply inferred from simultaneous methane and oxygen or nitrogen concentration measurements.

The effective saturation concentration can be expressed as an "effective depth," or the depth at which a bubble would be held under hydrostatic pressure to have the same equilibrium concentration as the effective saturation concentration. This depth could be compared with tail water depth, specific discharge, head, etc., at given structures. It will be used for comparison with these parameters because of the perspective it gives relative to tail water depth. The effective depth is computed as:

$$D_{eff} = K_p\left(\frac{C_{se} \cdot H}{comp} - P_{atm}\right) \tag{13}$$

where

D_{eff} = Effective bubble depth, m or ft

K_p = Conversion constant from atmosphere to depth of water (≈33.9 ft H_2O/atm or 10.34 m H_2O/atm), assuming hydrostatic pressure

C_{se} = Effective saturation concentration of oxygen or nitrogen, mg/ℓ, from Equation 12

H = Henry's Law coefficient for oxygen or nitrogen (atm ℓ/mg)

$comp$ = Fraction of gas in atmosphere (0.2095 for oxygen and 0.7808 for nitrogen)

P_{atm} = Barometric pressure, atm

Impact of Assuming a Zero Saturation Concentration for Methane

Equation 7 assumes the saturation concentration of methane is small since the concentration of methane in the atmosphere is essentially zero. However, the concentration of methane in a bubble may not approximate zero due to methane transferring into the bubble from the water as the bubble is dragged

through the plunge pool. Assuming all methane transfer occurs across a bubble interface, a mass balance of methane across the hydraulic structure is written as:

$$C_m = \frac{q_w}{q_a}(C_u - C_d) \tag{14}$$

where

C_m = Concentration of methane in a bubble as it is released to atmosphere

q_w = Unit discharge of water, m^2/sec

q_a = Unit entrainment of air, m^2/sec

C_u = Concentration of methane in water upstream of structure

C_d = Concentration of methane in water downstream of structure

Measurements taken at the Rum River gated OG spillway were used to assess the impact of assuming a methane saturation concentration of zero. C_u and C_d were measured at 16.58 and 8.72 mg/m^3(ppb), respectively. q_w was calculated from the gate opening, head, and geometry of the structure to be 0.167 m^2/sec. The specific discharge of the entrained air was measured directly using a 1- by 1-m square hood designed and built by Mr. Steven C. Wilhelms. The hood was placed on the water surface in the plunge pool capturing the air released to the atmosphere by the bubbles. The hood constricted into a 2-cm-diam pipe, where a hot film anemometer was placed to measure velocity, enabling the air discharge coming out of the water to be calculated. These measurements are given in the Appendix A. The hood was moved laterally and longitudinally along the tailrace in the region where air bubbles were escaping and the air flow rates were summed to yield the total air discharge. The specific air discharge was then calculated. For this experiment, q_a was computed from these measurements to be 0.125 m^2/sec.

Then, using Equation 14 to compute the released concentration of methane for a bubble:

$$C_m = \frac{0.167(m^2/\text{sec})}{0.125(m^2/\text{sec})}(16.58 - 8.72)mg/m^3 = 10.5mg/m^3 \tag{15}$$

The equilibrium concentration of methane, C_{me}, in a bubble downstream of the structure can be found from the Henry's Law relationship:

$$C_{me} = C_d \cdot H_{CH_4} \tag{16}$$

where H_{CH4} = dimensionless Henry's Law constant for methane = 17.98 at 0 °C. Using Equation 16 to calculate C_{me}:

$$C_{me} = 8.72\ mg/m^3\ (17.98) = 156.8\ mg/m^3 \tag{17}$$

Therefore, the concentration of methane in a bubble as it is released to the atmosphere is 6.7 percent of the equilibrium concentration of methane in that bubble.

The transfer efficiency of methane can be calculated by rewriting Equation 6 in terms of Henry's Law constant:

$$E_m = \frac{C_d - C_u}{\left(\frac{C_b}{H_{CH_4}}\right) - C_u} \tag{18}$$

where C_b is an average value of the methane concentration in the bubble, or:

$$C_b = \left(\frac{1}{2}\ C_m\right)\left(1 + \frac{D_{eff}}{10.3}\right) \tag{19}$$

The concentration of methane in the bubble varies as the bubble is washed through the plunge pool. At the inception of the bubble, the concentration is approximately zero, since there is relatively little methane in the atmosphere. As the bubble is released to the atmosphere at the end of the plunge pool, the concentration is C_m. The first term in Equation 19 is an arithmetic mean of the end point concentrations. The second term of Equation 19 accounts for the increase in concentration due to the reduction in volume of a discrete bubble as it is dragged to some depth in the plunge pool. For the example used herein, D_{eff} was computed from a comparison of oxygen and methane transfer measurements to be 0.8 m.

Solving Equations 18 and 19:

$$E_m = \frac{8.72-16.58}{\left(\frac{5.7}{17.98}\right) - 16.58} = 0.48 \tag{20}$$

$$C_b = \frac{1}{2}\ (10.5)\left(1 + \frac{0.832}{10.3}\right) = 5.7\ mg/m^3 \tag{21}$$

When the concentration of methane in a bubble is ignored, $C_s = 0$ and Equation 7 becomes:

$$E_m = \frac{8.72-16.58}{-16.58} = 0.47 \tag{22}$$

Thus, the difference in transfer efficiencies calculated by accounting for a concentration of methane in the bubble and by ignoring the concentration of methane in the bubble is only 1.9 percent of the transfer efficiency. This is well within the uncertainty of the measurements and was incorporated as a bias uncertainty in the calculations.

Further calculations using a predictive relationship for the q_a (Ervine and Elsawy 1975) calibrated to these measurements for entrained air discharge indicated that the bias of roughly 2 percent would apply to all discharges at this structure.

4 Sampling Technique

Oxygen and methane measurements were taken at all of the structures tested. Additionally, total dissolved gas measurements were taken at the Rum River structure to determine dissolved nitrogen concentration. At each site, an upstream sampling location was chosen as close to the structure as possible to ensure that the water sampled was representative of the water passing over the structure. The downstream sampling point was chosen close to the structure, yet downstream of the air entrained or bubbly region of the plunge pool. At both upstream and downstream sampling points, measurements were taken near the water surface, at mid-depth, and near the bottom to check for stratification of methane or oxygen.

Dissolved Oxygen Sampling

Dissolved oxygen measurements were performed in situ with a YSI No. 58 dissolved oxygen probe and meter. The probe was lowered to the appropriate sampling depth along a weighted tether to the probe from drifting to the surface in locations of high stream velocity. The meter reading of either concentration (mg/ℓ) or percent of saturation was recorded. The saturation concentration, C_s, was determined as:

$$C_s = \frac{0.0295\ P_{atm}}{H} \tag{23}$$

where H is Henry's Law and P_{atm} is atmospheric pressure. Gulliver and Rindels (1986) found the actual saturation concentration in river water to be 98 ± 2 percent of the values listed in the literature.

Total Dissolved Gas Sampling

The total dissolved gas concentration was measured in situ at the Rum River structure using a modified "gasometer" (Bouck 1982) consisting of a gas permeable tubing connected to a pressure transducer as shown in Photo 1. The

gasometer was also lowered to the appropriate depth along the weighted tether. After allowing the gasometer to equilibrate, the voltmeter reading from the pressure transducer was recorded. In most cases, it took approximately 15 to 20 min for the gasometer to equilibrate. The transducer was calibrated before each field trip to yield a known pressure for a given signal, as shown in Figure 5. The scatter of the calibration points shown in Figure 5 is within the range of uncertainty reported by the manufacturer. The slope of the calibration was determined from linear regression and the uncertainties reported by the manufacturer were included in the uncertainty of our measurements.

The dissolved nitrogen concentration, C_{N_2}, was computed as:

$$C_{N_2} = \frac{P_{N_2}}{H_{N_2}} \tag{24}$$

where H_{N_2} is the Henry's Law constant for nitrogen and P_{N_2} is the partial pressure of nitrogen inside the tubing calculated as:

$$P_{N_2} = 98.77\% \ (P - P_{O_2} - P_{H_2O}) \tag{25}$$

where P is the total dissolved gas pressure (measured with the gasometer), P_{H_2O} is the vapor pressure of water, and P_{O_2} is the partial pressure of oxygen in the tubing calculated as:

$$P_{O_2} = O_2\% \ (P_{atm} - P_{H_2O}) \ O_2 \textit{mole fraction in dry air} \tag{26}$$

where O_2 percent is the percent saturation of oxygen in the water, P_{atm} is the barometric pressure, and P_{H_2O} is the vapor pressure of water. The mole fraction of oxygen in dry air is 0.2095 (Weast 1976).

Methane Sampling

Methane sampling was performed by collecting water samples in the field and later analyzing those samples in the laboratory using the headspace analysis technique (described in Section VI). Water samples were collected in 40-mL borosilicate glass vials with Teflon-faced septa and open-top screw caps. The uncapped empty vials were loaded in the sampling device shown in Photo 2. The sampler was rapidly lowered to the appropriate depth. Water enters the sampler through the side tubings, and air exits the sampler through the top tube. This design virtually eliminates bubbling within the sampler that could result in stripping of methane from the water. Once filled, the sampler was removed from the water. The vials were capped, Teflon side down, under water while still in the sampler in order to reduce the volatilization of methane to the atmosphere. The capped samples were packed top down to prevent the

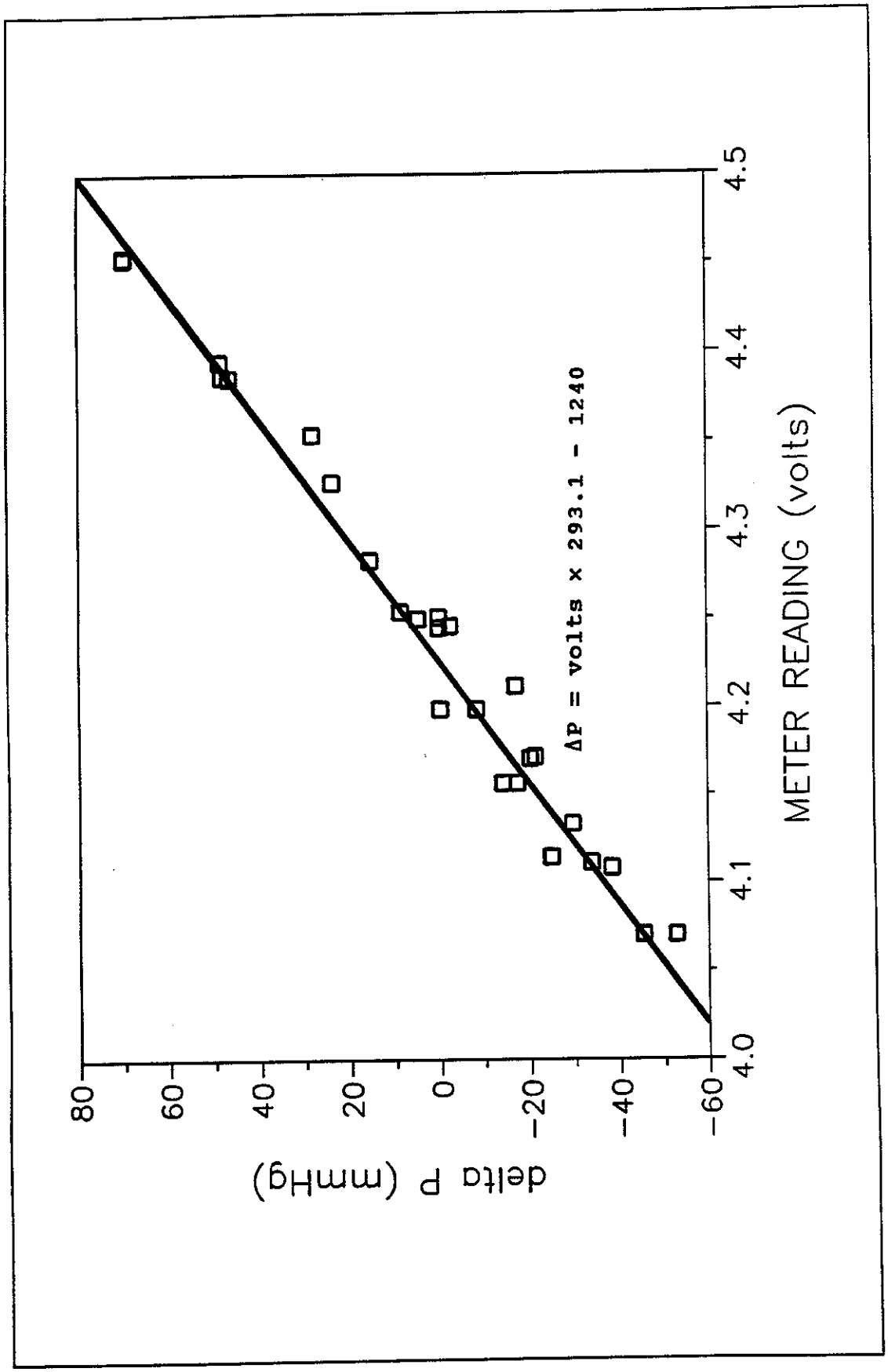

Figure 5. Total gas meter calibration

loss of methane due to bubble formation caused by temperature change and subsequent leakage through the septa or cap.

Sample preservation

As samples were not analyzed immediately after they were gathered, some method of preservation had to be employed. Schultz et al. (1971) concluded that 1 mL of 37-percent formalin solution in a 60-mL solution preserved the sample for 7 days. To stop bacterial action, other researchers have raised the pH to 11, added HgCl or stored samples on ice. It was decided to test 0.5 and 0.25 mL of 37-percent formalin solution to preserve the samples. Samples were gathered from the Anoka Dam on the Rum River and from the Mississippi River in Minneapolis. As can be seen from Figure 6, the methane concentrations with 1/4-mL formalin and with no formalin decreased with time. The samples with 1/2-mL formalin were relatively constant. Therefore, it was decided to use 1/2 mL of formalin as a preservative for this study. The formalin was injected in the samples as soon as possible after collection and before transport.

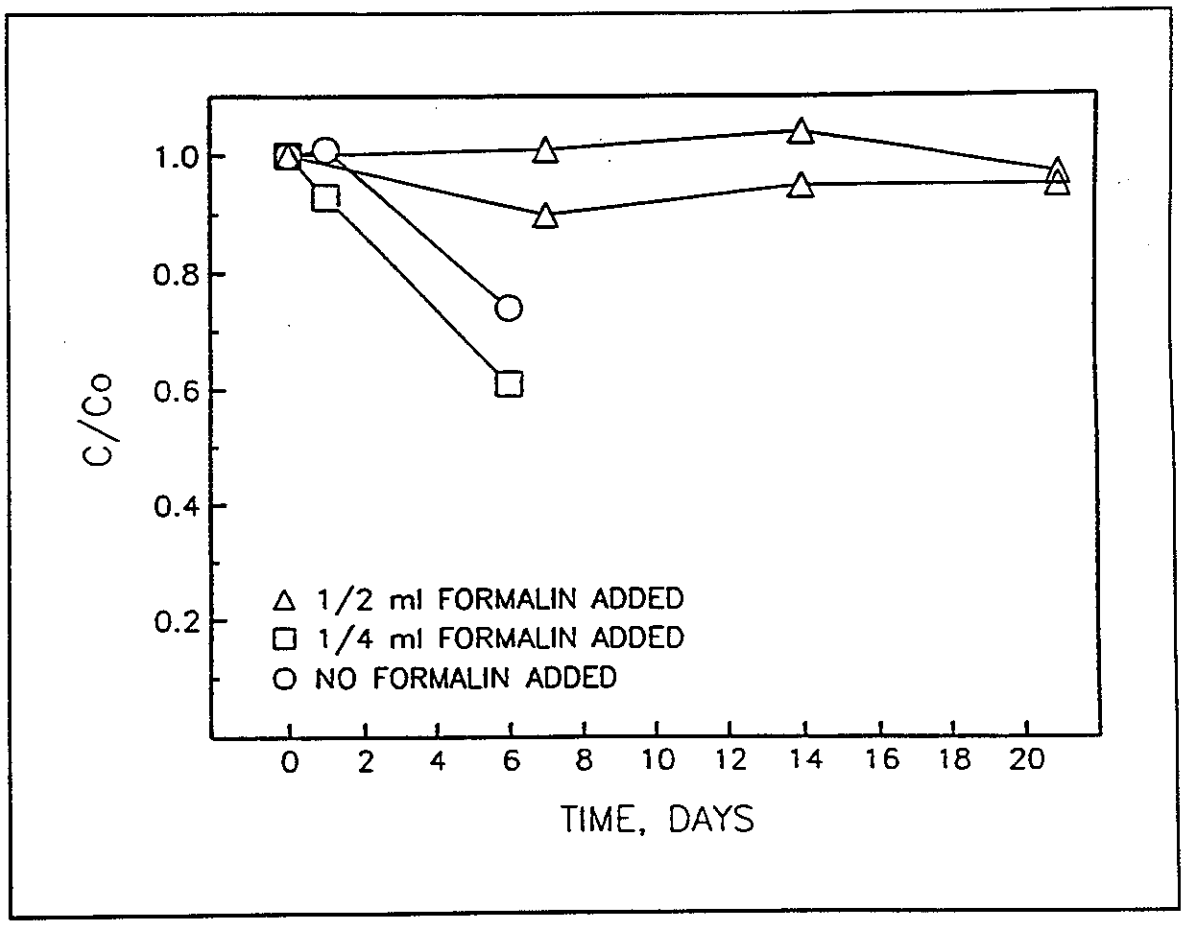

Figure 6. Effect of formalin on methane concentration

Sample transporting

The samples were transported to the gas chromatograph (GC) laboratory at the University of Minnesota, Department of Civil and Mineral Engineering for analysis. Samples obtained near the University were transported immediately by car, whereas samples obtained elsewhere were shipped via overnight express couriers.

All water samples collected at a given location exhibited a certain degree of precision uncertainty in methane concentration. However, those samples shipped by overnight couriers exhibited such a large precision uncertainty in methane concentration that for all practical purposes the samples were useless. Tables 1 and 2 show that sample vials collected at the same location and time, and even from the side by side bottles in the same sampler grab, varied in methane concentrations by as much as 69 percent. While there is a possibility that this is truly representative of the actual concentrations, it is extremely unlikely that there is that much of a variation in methane concentrations due to the turbulent mixing at structures. A more likely explanation for the large variances in concentrations is that there was a depletion of methane from some of the sample vials during shipping.

Although the samples were packed upside down, there is no way of knowing if the samples remained upside down for their entire journey to Minneapolis. Perhaps bubbles of high methane concentration formed and leaked out the bottle-septa seal or through a piercing hole in the septa while inverted. The potential for methane loss during transport is increased by the atmospheric pressure drop exerted on the samples during airplane transport. Figure 7 shows possible methane evasion routes. In light of the methane concentration randomness of the samples transported by air freight, an alternative method of transport is clearly needed.

Alternative sample shipping technique

An alternative packing and shipping technique has been developed and is currently being tested. The technique is referred to as the "double redundancy technique." The basis of the technique is that the sample vials are packed upside down immersed in a water bath. The technique is doubly redundant since first the risk of the of the inverted sample being righted is reduced. The package handlers will be less likely to tip over a package labeled "↑ LIQUID-THIS END UP ↑" in order to avoid a spill (actually, a spill would be very unlikely due to the watertight packaging). Secondly, even if the sample vials are righted, there is less potential for methane escape due to the vials being packed in a water bath. Figure 8 shows the restricted flow through a potential leak in a septa. The surface tension of the water on the outside face of a septa will prohibit the flow of gas from an air bubble on the bottle side of a septa.

Table 1
Methane Concentrations, Opekiska Lock and Dam, September 24, 1992

Location	Gate Opening ft	Sample Depth ft	Time of Sampling	Bottle No.	$[CH_4]$[1] µg/ℓ
Upstream	0.3	15	8:30	32	8.22 ± 0.44
				31	8.43 ± 1.36
				23	7.78 ± 0.33
				24	8.61 ± 3.32
		10	15:12	71	11.39 ± 3.17
				72	14.08 ± 2.92
				46	9.73 ± 0.52
Downstream	0.1	5	9:20	43	5.65 ± 0.09
				45	5.18 ± 0.28
				15	5.30 ± 0.41
				38	6.17 ± 0.12
	0.3	5	9:00	17	6.14 ± 0.05
				35	5.69 ± 0.34
				29	5.55 ± 0.14
				33	5.29 ± 0.03
	0.5	5	9:35	36	5.38 ± 0.18
				58	6.39 ± 0.49
				42	5.40 ± 0.42
				50	4.98 ± 0.05
	0.75	5	13:30	39	5.10 ± 0.48
				40	4.37 ± 0.14
	1.0	5	13:40	48	4.17 ± 0.07
				47	5.17 ± 0.53
				56	4.33 ± 0.20
				64	4.59 ± 0.17
	1.5	5	13:55	54	5.14 ± 0.83
				55	4.22 ± 0.25
				70	3.95 ± 0.06

(Continued)

[1] Uncertainties include only precision uncertainty.

Table 1 (Concluded)

Location	Gate Opening ft	Sample Depth ft	Time of Sampling	Bottle No.	$[CH_4]$ µg/ℓ
Downstream	1.5	5	13:55	62	4.57 ± 0.19
	2.0	5	14:10	60	4.67 ± 0.13
				68	5.30 ± 0.48
				63	5.37 ± 0.15
				61	5.51 ± 1.34

Table 2
Methane Concentrations, Smithland Lock and Dam, September 23, 1992

Location	Gate Opening ft	Sample Depth ft	Time of Sampling	Bottle No.	$[CH_4]$[1] µg/ℓ
Upstream	2.0	15	11:57	30	3.08 ± 0.09
				22	2.89 ± 0.19
				41	3.58 ± 0.29
				49	2.75 ± 0.14
Downstream	0.5	15	9:40	9	10.22 ± 0.54
				10	7.66 ± 0.55
				12	12.16 ± 0.49
	1.0	15	10:05	6	7.17 ± 0.08
				14	6.63 ± 0.75
				7	6.95 ± 0.20
				16	7.33 ± 1.32
	1.5	15	10:25	13	5.55 ± 0.59
				25	6.06 ± 0.87
				5	6.71 ± 0.47
	2.0	15	10:55	20	6.74 ± 0.56
				21	6.58 ± 0.56
			11:00	35	5.14 ± 0.28
				28	5.44 ± 0.30

[1] Uncertainties include only precision uncertainty.

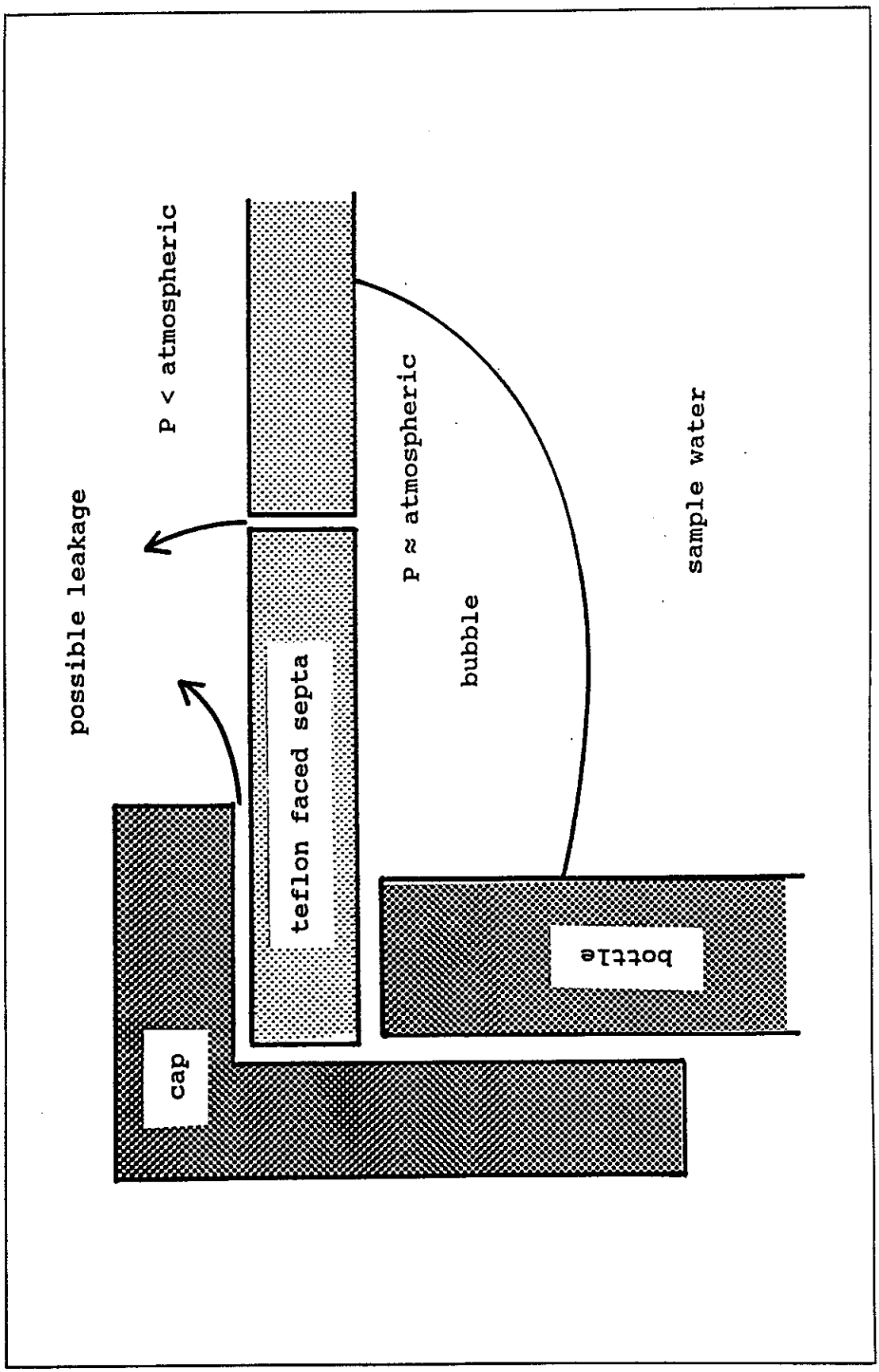

Figure 7. Potential evasion routes of methane during sample transport

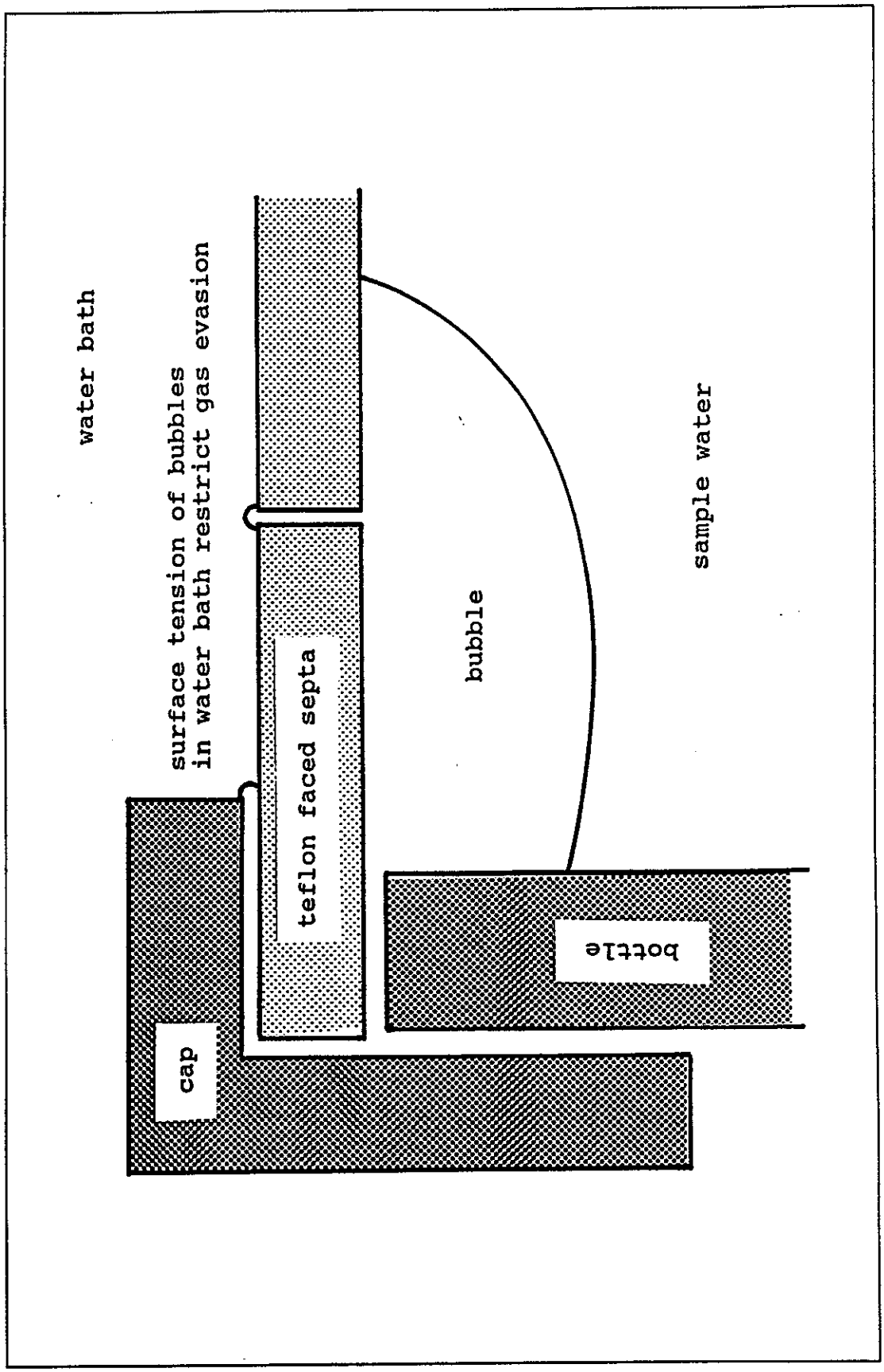

Figure 8. Restricted flow of gas from sample immersed in water bath

In practice, an empty 1-gal[1] paint can could be used as the container. The vials could be cushioned with sponge or foam packing. The packing would also serve as a spacer to keep the septa of all vials below the water surface inside the can, regardless of the upward orientation of the can. No results on the effectiveness of the technique are available as of this writing since the technique is currently being tested.

[1] A table of factors for converting non-SI units of measurement to SI (metric) units is presented on page viii.

5 Headspace Analysis Technique

A slightly modified version of the headspace analysis technique developed by Thene and Gulliver (1990) was used to determine the concentration of methane in the water samples by measuring the methane concentration of the air in equilibrium with the water.

Calculation of Methane Concentration in Water

The concentration in the headspace, C_a, is given by Thene and Gulliver (1990) as:

$$C_a = C\left[\frac{RT}{MH}+\frac{V_a}{V_w}\right]^{-1} \tag{27}$$

where

C = Concentration in the water prior to the creation of the headspace

R = Universal gas constant

T = Water temperature

M = Molar mass of methane

H = Henry's Law constant for methane

V_a = Volume of headspace in sample bottle

V_w = Volume of water in sample bottle

The exact volumes of headspace and water in the samples used in Equation 27 were determined by weighing each bottle before creating the headspace, after creating the headspace, and when empty.

Creating the Headspace

A headspace was created in each sample vial at the GC laboratory. Photo 3 shows the method used to make the headspaces. A drainage needle open to the atmosphere was inserted in the septa of the upside down vial. Approximately 10 mL of nitrogen gas were injected through the septa at the top of the vial, forcing water out through the drainage needle. Samples were then shaken vigorously for 60 sec to strip the methane from the water into the headspace.

Gas Chromatography

The gas chromatograph (GC) used was a Hewlett Packard 5890A equipped with a flame ionization detector (FID), a strip chart recorder, and an electronic integrator and a 4-ft-long 5A 60/80 molecular sieve.

Five separate 200-µℓ volumes were withdrawn from the headspace of each bottle with a 250-µℓ gas-tight syringe and then injected into the GC. At least three injections were needed to accurately compute the precision uncertainty of the measurement; five was chosen as a matter of convenience. The pressure in the headspace was kept nearly constant by counter-injecting 200 µℓ of water into the sample prior to withdrawal of the GC injection.

The water used to replace the sample volume must not contain methane. Headspace analysis of de-ionized water, tap water, and Mega-Pure water showed that only the Mega-Pure water sample did not give a GC response. Therefore, only Mega-Pure water was used to replace the extracted 200-µℓ volumes. The injection of 1 mL of Mega-Pure water does slightly affect the methane concentration of the headspace. However, the effect is small due to methane's high volatility (McDonald and Gulliver 1992; Thene and Gulliver 1990).

Calibration of the GC was performed by injecting different volumes of 100 ppm (by volume) methane standard and plotting the results. A curve was then fit through the calibration points to obtain an equation relating area count to mass of methane, as shown in Figure 9. This mass was then related to concentration in the original sample as described in McDonald and Gulliver (1992). Uncertainties in the concentration measurements were also computed to the 95-percent confidence interval. The confidence interval was typically ±1 to 2 percent of the measured concentration.

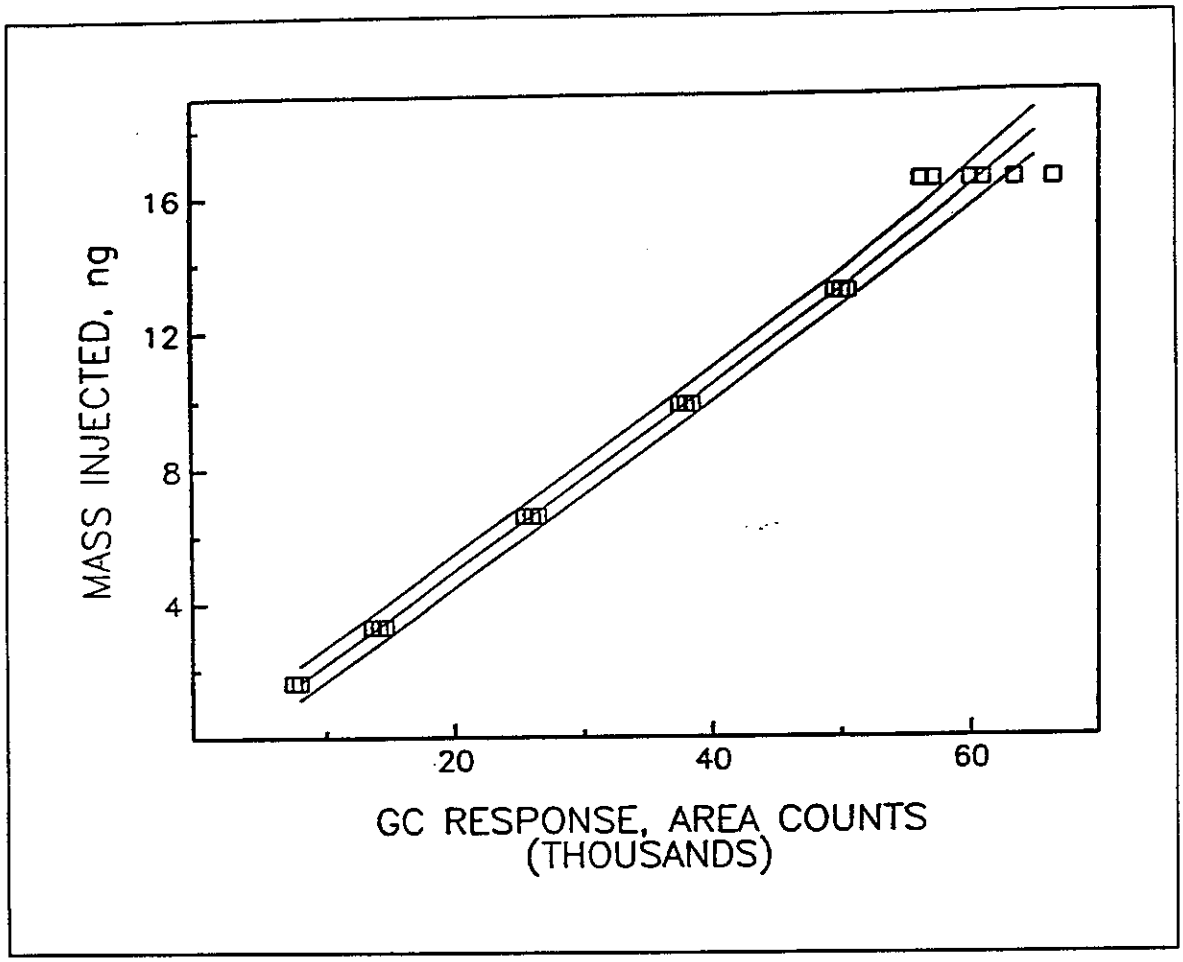

Figure 9. GC Calibration

A quality control/quality assurance program was also carried out to ensure that the concentrations in the water column were, within the confidence limits, correctly determined from the GC readings. Tests were performed on the length of time the samples could be preserved, the quantity of formalin required for preservation, the technique of sample injection into the GC, the impact of headspace pressure change due to sampling, the GC response of formalin, the reuse of septa, and the effect of bubble formation in the vials (McDonald and Gulliver 1992).

Injection technique

It was discovered that the speed in which the sample was injected into the GC led to different responses. To test the effects of injection speed, different volumes of standard were injected into the GC at different speeds. Three speeds were tested. The first speed was to inject as fast as possible. The total time to pierce the septa, depress the plunger, and withdraw the syringe was under 0.5 sec. The second speed was a 3-sec process. One second was used

to pierce the septa and to get the syringe in place. Two seconds were used to depress the plunger; then the syringe was withdrawn quickly. The third speed tested was similar to the second; only 4 sec total were required for the entire injection process. As shown in Figure 10, the fast injection yields a different response from the other injection speeds. Thus, if the injection speed is 0.6 sec instead of 0.5 sec, the results could be different. The other two plots are virtually identical, indicating that the results were very nearly insensitive to injection speed for the 3- and 4-sec injection. Therefore, it was decided to use the 3-sec injection for samples. It is thought with the fast injection that some of the sample is lost through the pierced septa in the injection port of the GC or through the plunger seal in the gas-tight syringe.

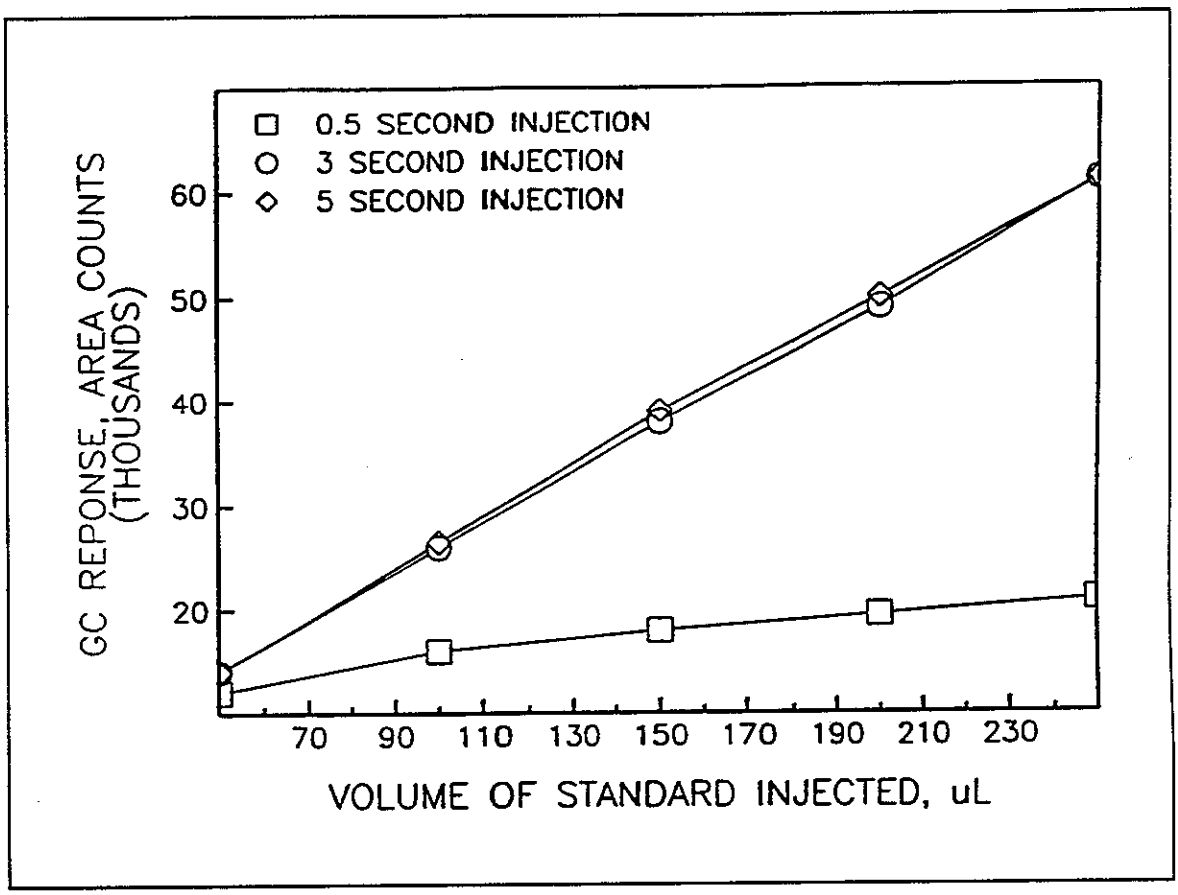

Figure 10. Impact of injection speed on GC response

Limit of detection/limit of quantification

The limit of detection, LOD, is defined as the lowest concentration that is statistically different from the blank. The limit of quantification, LOQ, is the concentration level above which quantitative results can be obtained with confidence. In most cases, the LOD and LOQ are defined as three and ten times the standard deviation of the response to blank runs, respectively (American Chemical Society 1983). Experience has shown that there is no "methane"

response to blank runs. Consequently, a different procedure was required. It was decided that an appropriate LOD and LOQ could be determined by injecting various masses of the standard gas each 10 times into the GC and calculating the standard deviation of each subset of injections. Then the LOQ was defined as the point where ten times the standard deviation of a set of injections equaled the average area count of the set of injections. Or LOQ = C when $C = 10\sigma$, where C is the mean concentration and σ the standard deviation in concentration measurements. Similarly, the LOD was defined as the point where three times the standard deviation equaled the average area count.

Using this definition and the information gathered from the injection of standard gas, Table 3 was prepared. This table shows the LOQ to lie between the mass contained in 3 and 5 µℓ of standard gas. By linear interpolation between these two points, the mass of LOQ was equal to 0.000211 µg.

Table 3
Data Used for LOQ Analysis

Volume, µℓ	Mass, µg	Mean AC	10 σ	10σ/mean	Equivalent Water Concentration, µg/ℓ
150	0.009963	35,045.1	5,539.3	0.16	14.7
100	0.006642	22,996.1	7,456.6	0.32	9.5
50	0.003321	12,192.9	4,356.6	0.36	4.9
10	0.000664	2,886.8	1,658.2	0.57	0.98
5	0.000332	1,891.4	1,118.3	0.59	0.49
3	0.000199	1,007.1	1,047.5	1.04	0.29

Assuming a 250-µℓ sample injection, the headspace concentration would be:

$$C_a = \frac{mass}{volume} = \frac{0.000211\mu g}{250\mu \ell} = 0.84\mu g/\ell \qquad (28)$$

Since the volume of headspace is roughly 10 mℓ and the volume of water is roughly 30 mℓ, the pre-headspace water concentration is computed from Equation 12 as:

$$C = (0.04+0.33)C_a = 0.37C_a = 0.3\mu g/\ell \qquad (29)$$

This is the value for LOQ. LOD is defined as 3/10 of the LOQ such that:

$$LOD = \frac{3}{10} LOQ = 0.1 \mu g/\ell \tag{30}$$

Bubble Formation

Bubbles may be formed in the samples as the samples are transported from cold temperatures to warmer temperatures. A calculation was thus made to determine if the bubbles formed would significantly affect the methane concentration in the sample. For this calculation, a 3-mm-diam bubble and a water methane concentration of C = 20 µg/ℓ were assumed. Equation 27 then becomes:

$$C_a = 20 \mu g/\ell \ (0.037 + 0.00036) = 535 \ \mu g/\ell \tag{31}$$

The percentage of the total methane in the sample bottle that is in the bubble, percent $CH_{4\ bubble}$, is:

$$percent\ CH_{4\ bubble} = 100 \frac{C_a V_a}{C V_w} = 0.96\ percent \tag{32}$$

The bubble would remain in the vial upon headspace injection and would become a part of the headspace. If 10 mL of water is removed, while 30 mL remain, the headspace concentration for this example would be high by 1/4(0.96 percent) = 0.24 percent. This percent difference is insignificant compared with the precision of the GC analytic technique for methane.

6 Results

The results of simultaneous methane-oxygen transfer at four structures are summarized in Table 4. Descriptions of the structures are included in Appendix B. Figure 11 shows the effective depth plotted versus specific discharge at Rum River for six separate field trips. Figure 12 is a similar plot for the St. Cloud structure on 15 March 1990 and 05 April 1993. The calculated effective depth at the Anoka structure is reproducible as a function of specific flow rates for a variety of water temperatures, upstream oxygen deficits, and heads. The effective depths at the St. Cloud differ from those at the Rum River structure for comparable specific discharges, perhaps due to differences in head, tail water depth, and plunge pool design.

Generally, as the specific discharge increases, the effective depth increases. At low discharges, the momentum of the plunging jet is insufficient to carry the bubbles deep into the pool, and the effective saturation concentration is close to local atmospheric concentration. At high discharges, the momentum of the plunging jet carries the entrained bubbles deeper into the pool, and the effective saturation concentration is significantly higher than that computed from local atmospheric concentration because of the higher pressures that the bubbles experience. Negative values of effective depth are listed in Table 4 for the lower discharges at the Kost and St. Cloud structures. There is no physical explanation for this. The actual effective depth values are most likely positive and the measurements are in error. In each case where a negative effective depth is calculated, there is a greater uncertainty in the reported effective depth. Thus, these negative values are small relative to the measurement uncertainty.

As a verification of the principles presented herein, effective depths were calculated from dissolved nitrogen measurements and from dissolved oxygen for a range of discharges, using methane as the tracer gas for both. Nitrogen and oxygen are both present in quantity in the atmosphere and therefore in the entrained bubbles. As a bubble is pulled to some depth in the plunge pool, the same hydrostatic forces increase the partial pressures of both oxygen and nitrogen proportionally to their atmospheric concentrations. This proportionally uniform increase in partial pressures leads to a proportionally uniform increase in the effective saturation concentrations, and ultimately a uniform increase in the effective depth. Thus, the effective depth calculated using dissolved

Table 4
Results of Simultaneous Methane and Oxygen Transfer Measurements at Various Hydraulic Structures (Uncertainty is given to the 95-percent confidence level)

Structure	q m^2/sec	Oxygen C_u mg/ℓ	Oxygen C_d mg/ℓ	Oxygen E	Methane C_u µg/ℓ	Methane C_d µg/ℓ	Methane E	D_{eff} m	Tail Water Depth m
St. Cloud-Gated	0.16	10.05	11.84	0.50 ± .05	7.95	4.20	0.47 ± .04	-0.3 ± 0.3	5.7
3/15/90	0.32	10.06	11.67	0.45 ± .04	7.95	4.00	0.50 ± .05	-0.6 ± 0.3	5.7
T_{water}=0.0 °C	0.63	10.07	12.08	0.56 ± .05	7.95	3.30	0.58 ± .08	-0.4 ± 0.3	5.8
O_2 C_s=13.63 mg/ℓ	1.27	10.09	12.45	0.67 ± .06	7.66	4.14	0.46 ± .08	0.6 ± 0.6	5.8
P_{atm}= 724.05 mmHg	2.09	10.11	12.28	0.62 ± .06	7.66	4.97	0.35 ± .08	1.3 ± 0.9	5.8
	2.93	10.13	10.67	0.15 ± .06	7.66	7.35	0.04 ± .08	6.0 ± 16.6	5.8
	3.61	10.15	10.79	0.18 ± .02	7.66	7.21	0.06 ± .07	4.2 ± 8.3	5.8
4/5/93	0.39	13.06	13.32	0.31 ± 0.13	4.48	2.71	0.40 ± 0.07	-0.4 ± 0.3	5.7
T_{water}=0.9 °C	0.79	13.06	13.51	0.52 ± 0.20	4.48	2.83	0.37 ± 0.07	-0.1 ± 0.3	5.8
O_2 C_s=13.92 mg/ℓ	1.18	13.06	14.09	1.19 ± 0.45	4.48	2.98	0.33 ± 0.07	1.1 ± 0.5	5.8
P_{atm}= 745.0 mmHg	1.58	13.06	14.35	1.50 ± 0.57	4.48	2.71	0.40 ± 0.07	1.2 ± 0.5	5.8
Rum River-Gated	0.16	8.05	11.97	0.67 ± 0.04	15.20	6.13	0.60 ± 0.04	1.0 ± 0.5	3.2
3/2/90	0.35	8.05	11.69	0.63 ± 0.03	15.20	7.63	0.51 ± 0.03	1.1 ± 0.5	3.3
T_{water}=0.1 °C	0.66	8.05	11.27	0.55 ± 0.03	15.20	10.1	0.33 ± 0.03	2.9 ± 0.8	3.3
O_2 C_s=13.86 mg/ℓ	1.26	8.05	10.97	0.50 ± 0.03	15.20	10.7	0.29 ± 0.03	3.2 ± 0.9	3.4
P_{atm}=738.4 mm Hg	1.81	8.05	10.65	0.45 ± 0.03	15.20	11.7	0.25 ± 0.02	3.4 ± 0.8	3.5
	2.3	8.05	10.44	0.41 ± 0.02	15.20	12.7	0.21 ± 0.02	4.1 ± 1.0	3.7

(Sheet 1 of 3)

Table 4 (Continued)

Structure	q m^3/sec	Oxygen C_u mg/ℓ	Oxygen C_d mg/ℓ	Oxygen E	Methane C_u µg/ℓ	Methane C_d µg/ℓ	Methane E	D_{eff} m	Tail Water Depth m
8/31/93	0.78	6.89	8.89	1.05 ± 0.11	7.48	3.23	0.57 ± 0.03	1.5 ± 0.2	3.4
T_{water}=19.6 °C	1.10	7.06	8.89	1.05 ± 0.12	7.48	3.36	0.55 ± 0.03	1.5 ± 0.3	3.4
O_2 C_s=8.80 mg/ℓ	1.42	7.11	8.93	1.08 ± 0.13	7.48	3.42	0.54 ± 0.03	1.6 ± 0.3	3.4
P_{atm}=742.8 mm Hg	1.73	7.16	8.93	1.08 ± 0.13	7.48	3.78	0.50 ± 0.03	1.9 ± 0.3	3.7
	2.36	7.32	8.67	0.91 ± 0.13	7.48	5.08	0.32 ± 0.05	2.7 ± 0.7	3.8
	3.15	7.36	8.56	0.84 ± 0.12	7.48	4.99	0.33 ± 0.03	2.1 ± 0.5	3.8
6/22/93	0.97	8.04	9.48	2.06 ± 0.60	5.31	2.31	0.56 ± 0.21	1.9 ± 1.0	3.6
T_{water}=19.9 °C	1.21	8.04	9.50	2.09 ± 0.61	5.31	2.56	0.52 ± 0.15	2.2 ± 0.8	3.7
O_2 C_s=8.74 mg/ℓ	1.82	8.04	9.55	2.16 ± 0.63	5.31	3.09	0.42 ± 0.20	3.0 ± 1.7	3.8
P_{atm}=742.8 mmHg									
Rum River-Gated	0.17	8.57	1.97	0.64 ± 0.04	16.58	8.72	0.47 ± .04	0.9 ± 0.5	3.3
2/17/90									
T_{water}=0.1 °C									
O_2 C_s=13.86 mg/ℓ									
P_{atm}=744.3 mmHg									
3/21/89	0.16	7.41	11.58	0.68 ± 0.03	16.25	8.10	0.50 ± 0.07	1.1 ± 0.8	3.4
T_{water}=1.0 °C									
O_2 C_s=13.58 mg/ℓ									

(Sheet 2 of 3)

Table 4 (Concluded)

Structure	q m^3/sec	Oxygen C_u mg/ℓ	Oxygen C_d mg/ℓ	Oxygen E	Methane C_u µg/ℓ	Methane C_d µg/ℓ	Methane E	D_{eff} m	Tail Water Depth m
P_{atm}=741.2 mmHg									
3/25/93	0.44	11.48	13.61	0.84 ± 0.11	16.61	9.92	0.40 ± 0.71	1.4 ± 5.8	3.4
T_{water}=0.1 °C									
O_2 C_s=14.02 mg/ℓ									
P_{atm}=746.5 mmHg									
Rum River-Free Weir		8.05	11.63	0.59 ± 0.03	15.13	7.66	0.49 ± 0.04	0.4 ± 0.8	0.6
3/2/90		11.63	12.00	0.15 ± 0.03	7.66	7.30	0.05 ± 0.04	3.2 ± 8.7	0.6
T_{water}=0.1 °C									
0_2 C_s=13.86 mg/ℓ									
P_{atm}=738.4 mm Hg									
Kost Dam-Free Weir	0.05	8.57	10.59	0.35 ± 0.02	54.01	33.30	0.38 ± 0.07	-0.6 ± 0.4	0.2
1/26/90	0.05	8.58	10.53	0.36 ± 0.02	48.48	34.49	0.29 ± 0.02	0.40 ± 0.08	0.2
T_{water}= 0.4 °C	0.05	9.34	11.01	0.36 ± 0.03	53.55	37.45	0.30 ± 0.06	0.3 ± 1.0	0.2
C_s=13.73 mg/ℓ									
P_{atm}=739.6 mm Hg									

(Sheet 3 of 3)

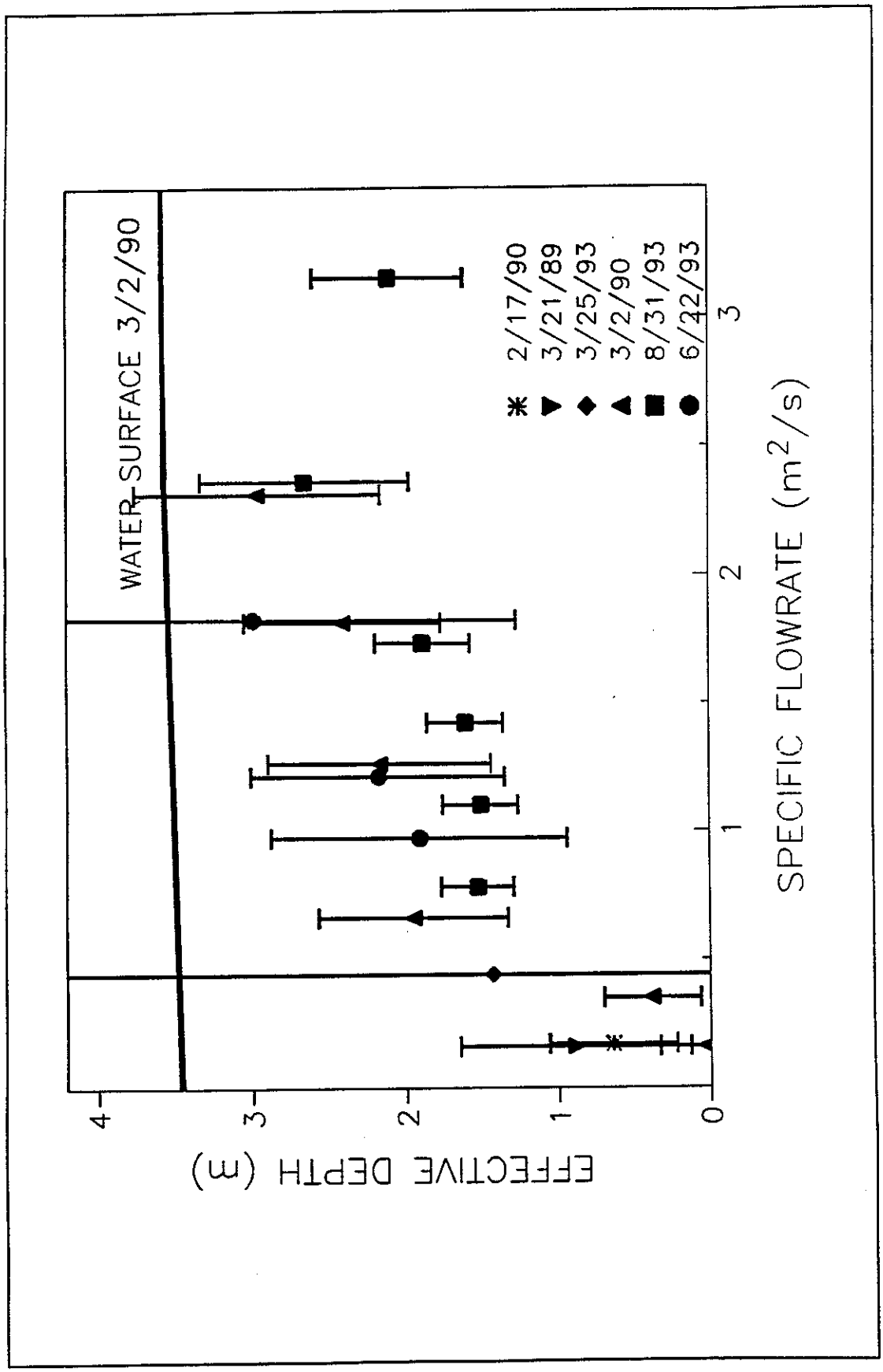

Figure 11. Effective depth versus specific discharge at Rum River Dam

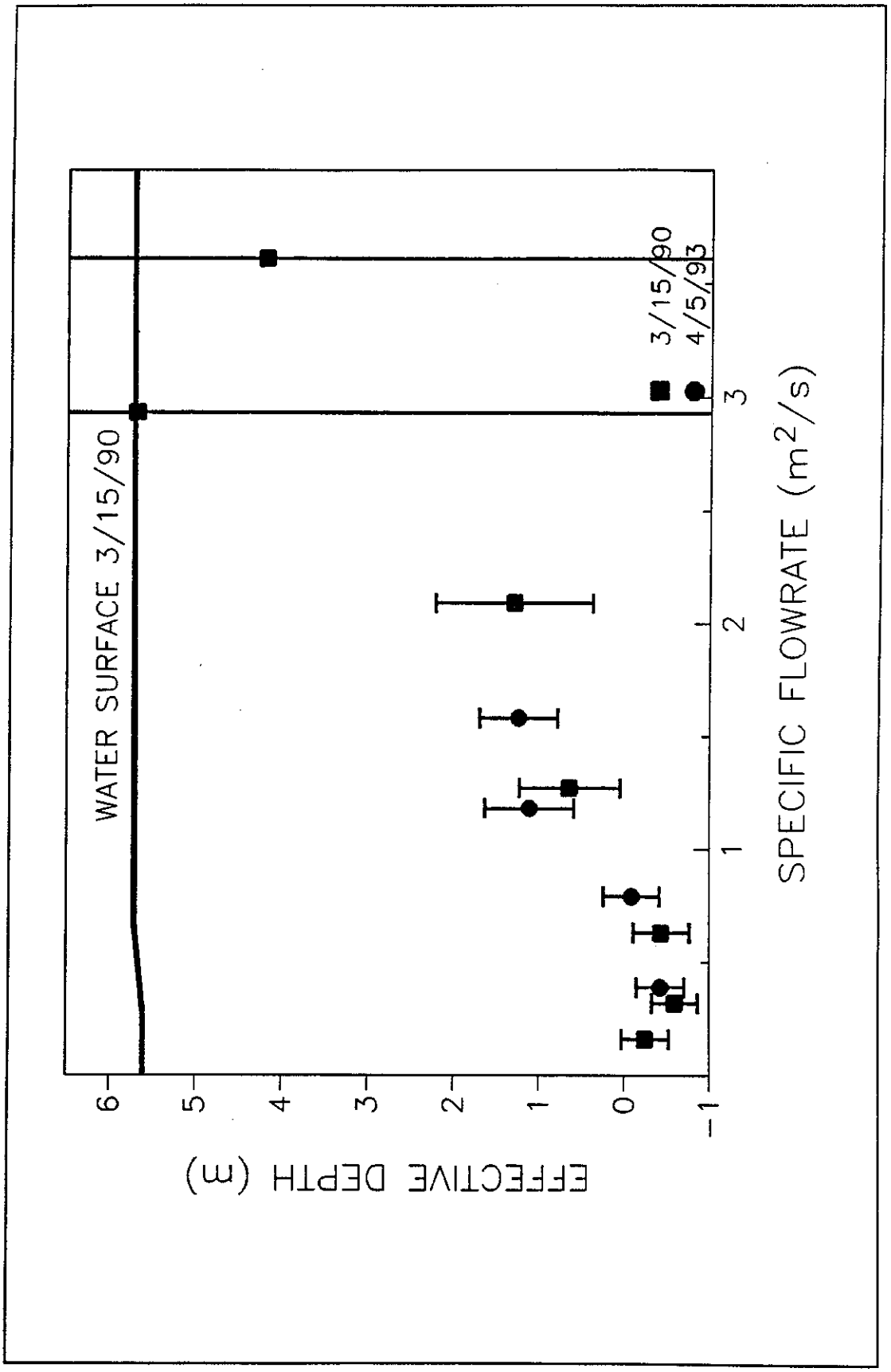

Figure 12. Effective depth versus specific discharge at St. Cloud Dam

nitrogen measurements should equal the effective depth calculated using dissolved oxygen measurements.

Table 5 shows the results of simultaneous methane, oxygen, and nitrogen transfer at the Rum River structure on 31 August 1993. At each specific discharge tested, the effective depth computed using dissolved nitrogen concentrations was found to be similar to the effective depth computed using dissolved oxygen data within the confidence interval of the measurement.

Table 5
Results of Simultaneous Methane, Oxygen, and Nitrogen Transfer Measurements at Rum River Dam, 13 August 1993

Water Temperature = 19.6°C
Tail water depth = 3.4 m
Barometric Pressure = 742.8 mmHg
O_2 Henry's Law constant = 17.78 mmHg·ℓ/mg
N_2 Henry's Law constant = 39.20 mmHg·ℓ/mg
O_2 saturation concentration = 8.74 mg/ℓ
N_2 saturation concentration = 14.72 mg/ℓ

	Methane			Oxygen			Nitrogen		
q m^2/sec	C_u[1] µg/ℓ	C_d[2] µg/ℓ	E	C_u[3] mg/ℓ	C_d mg/ℓ	D_{eff}[2] C_u m	C_d mg/ℓ	D_{eff}[2] mg/ℓ	m
0.78	7.48	3.23 ± 0.05	0.57 ± 0.03	6.89	8.89	1.53 ± 0.24	14.72	16.42	1.78 ± 0.39
1.10	7.48	3.36 ± 0.04	0.55 ± 0.03	7.06	8.89	1.51 ± 0.25	14.72	16.02	1.38 ± 0.40
1.42	7.48	3.42 ± 0.01	0.54 ± 0.03	7.11	8.93	1.61 ± 0.25	14.72	16.09	1.49 ± 0.40
1.73	7.48	3.78 ± 0.08	0.50 ± 0.03	7.16	8.93	1.89 ± 0.31	14.72	16.19	1.76 ± 0.46
2.36	7.48	5.08 ± 0.23	0.32 ± 0.05	7.32	8.67	2.65 ± 0.68	14.72	16.24	2.82 ± 0.83
3.15	7.48	4.99 ± 0.03	0.33 ± 0.03	7.36	8.56	2.10 ± 0.49	14.72	16.29	2.81 ± 0.75

[1] Uncertainty in upstream methane concentration is 0.29 µg/ℓ.
[2] Uncertainties are given to the 95-percent confidence level.
[3] Assumes a linear increase in upstream DO over data collection period.

7 Conclusions

The following conclusions were drawn from this study.

a. Measurement of in situ methane concentration is a viable technique for determining the transfer efficiency across a hydraulic structure or any device having a large rate of gas transfer and a relatively short residence time. It may also have other applications, such as measuring transfer efficiency in pneumatic diffusers.

b. Methane is usually not stratified in shallow reservoirs (less than 8 m deep) except under ice cover, where methane was found to be strongly stratified.

c. Because methane stratification in deeper reservoirs increases the uncertainty in determining the mean methane concentration at the top of the hydraulic structure, the methane tracer technique is most applicable to low head structures.

d. Oxygen and methane transfer efficiencies were found to be different when atmospheric pressure was used to compute oxygen saturation concentration and significant entrainment of air into the tail water pool occurred. This difference is believed to occur because entrained air bubbles pulled to a depth of higher pressure in the tail water results in a larger saturation concentration for oxygen, while methane saturation is essentially zero throughout. This is a source of error in using the transfer efficiency of tracers to compute oxygen transfer efficiency and in using the measured oxygen transfer efficiencies to compute the transfer efficiencies of other compounds of interest, such as the many volatile toxic compounds in surface waters.

e. Simultaneous oxygen-methane transfer measurements and nitrogen-methane transfer measurements have been used to compute an effective saturation concentration that is a weighted mean of the saturation concentration that a submerged bubble experiences in its path through a hydraulic structure and plunge pool. The measurements have also been used to compute a similarly weighted mean depth of bubble penetration, called the effective depth, at two-gated control structures.

f. Generally, as discharges increase, the effective depth increases, due perhaps to the increase momentum pulling the bubbles deeper in the plunge pool.

g. Measurements were used to compute the effective depth as a function of specific discharge on three different days at one structure. At comparable discharges, the effective depths were found to be similar within the confidence interval of the measurements.

h. The effective depth computed from oxygen-methane measurements was similar to that computed from nitrogen-methane measurements within the confidence interval of the measurements for a range of specific discharges at a structure, thus verifying the concept of effective depth.

i. More of these measurements need to be performed at other structures to relate the effective depth to parameters of the jet and structure. Only then can full use of gas transfer measurements be made at hydraulic structures.

References

Abram, J. W., and Nedwell, D. B. (1978). "Inhibition of methanogenesis by sulfate reducing bacteria competing for transferred hydrogen," *Archives of Microbiology* 117, 89-92.

American Chemical Society. (1983). "Principals of environmental analysis," *Analytical Chemistry* 55, 2210-2218.

de Angelis, M. A., and Lilley, M. D. (1987). "Methane in surface waters of Oregon estuaries and rivers," *Limnology and Oceanography* 32(3), 716-722.

Bouck, G. R. (1982). "Gasometer: An inexpensive device for continuous monitoring of dissolved gases and supersaturation," *Transactions of the American Fisheries Society* 111, 505-516.

Ervine, D. A., and Elsawy, E. M. (1975). "The effect of a falling nappe on river aeration," *Proceedings XVI Congress, Int'l. Association for Hydraulic Research*, IAHR, Delft, The Netherlands, Vol. 3, 390-397.

Ervine, D. A., and Falvey, H. T. (1987). "Behavior of turbulent waterjets in the atmosphere and in plunge pools," *Proceedings, Inst. of Civil Engineers*, Vol. 83, No. 2, 295-314.

Gulliver, J. S., Thene, J. R., and Rindels, A. J. (1990). "Indexing gas transfer in self-aerated flows," *ASCE, Journal of Environmental Engineering* 116(3), 503-523.

Gulliver, J. S., and Wilhelms, S. C. (1992). "Discussion of aeration at Ohio River Basin navigation dams," ASCE, *Journal of Environmental Engineering* 118(3), 444-446.

Gulliver, J. S., and Rindels, A. J. (1993). "Measurement of air-water oxygen transfer at hydraulic structures," ASCE, *Journal of Hydraulic Engineering*.

Hanratty, T. J. (1991). "Effect of gas flow on physical absorption." *Air-water mass transfer*. S. C. Wilhelms and J. S. Gulliver, ed., ASCE, New York, 10-13.

Johnson, P. L. (1984). "Prediction of dissolved gas transfer in spillway and outlet works stilling basin flows." *Gas transfer at water surfaces.* W. Brutsaert and G. H. Jirka, ed., D. Reidel Publishing Company, Boston, MA, 605-612.

Lovley, D. R., Dwyer, F., and Klug, M. J. (1982). "Kinetic analysis of competition between sulfate reducers and methanogens for hydrogen in sediments," *Applied and Environmental Microbiology* 43(6), 1373-1379.

McCutcheon, S. C. (1989). *Water quality modeling, Vol. 1: Transport and surface exchange in rivers.* CRC Press, Boca Raton, FL.

McDonald, J. P., and Gulliver, J. S. (1992). "*Methane tracer technique for gas transfer at hydraulic structures*," St. Anthony Falls Hydraulic Laboratory Project Report 325, University of Minnesota, Minneapolis, MN.

National Research Council. (1929). *International Critical Tables.* Vol. III, McGraw-Hill, Inc., New York.

Rathbun, R. C., Stephens, D. W., Schultz, D. J., and Tai, D. Y. (1978). "Laboratory Studies of gas tracers for reaeration," *Journal of Environmental Engineering Division*, ASCE, 104(EE2), 1215-1220.

Rathbun, R. E. (1990). "Prediction of stream volatilization coefficients," ASCE, *Journal of Environmental Engineering* 116(3), 615-631.

Strayer, R. F., and Tiedge, J. M. (1978). "In situ methane production in a small, hypereutrophic, hard-water lake: Loss of methane from sediments by vertical diffusion and ebullition," *Limnology and Oceanography*, 28(6), 1201-1206.

Thene, J. R., and Gulliver, J. S. (1990). "Gas transfer measurements using headspace analysis of propane," *Journal of Environmental Engineering*, 116(6), 1107-1124.

Tsivoglou, E. C. (1968). "Tracer measurement of stream reaeration: II. Field studies," *Journal of the Water Pollution Control Federation* 77(2), 219-262.

Weast, R. C., ed. (1976). *Handbook of chemistry and physics 57th edition.* CRC Press, Cleveland, OH.

Wetzel, R. G. (1975). *Limnology.* W. B. Sanders Co., Philadelphia, PA.

Wilhelms, S. C., Gulliver, J. S., and Parkhill, K. (1993). "Reaeration at low-head structures," Technical Report W-93-?, U.S. Army Engineer Waterways Experiment Station, Vicksburg, MS.

Zeikus, J. G., and Winfrey, M. R. (1976). "Temperature limitation of methanogenesis in aquatic sediments," *Applied and Environmental Microbiology* 31(2), 99-107.

Photo 1. Total dissolved gas meter

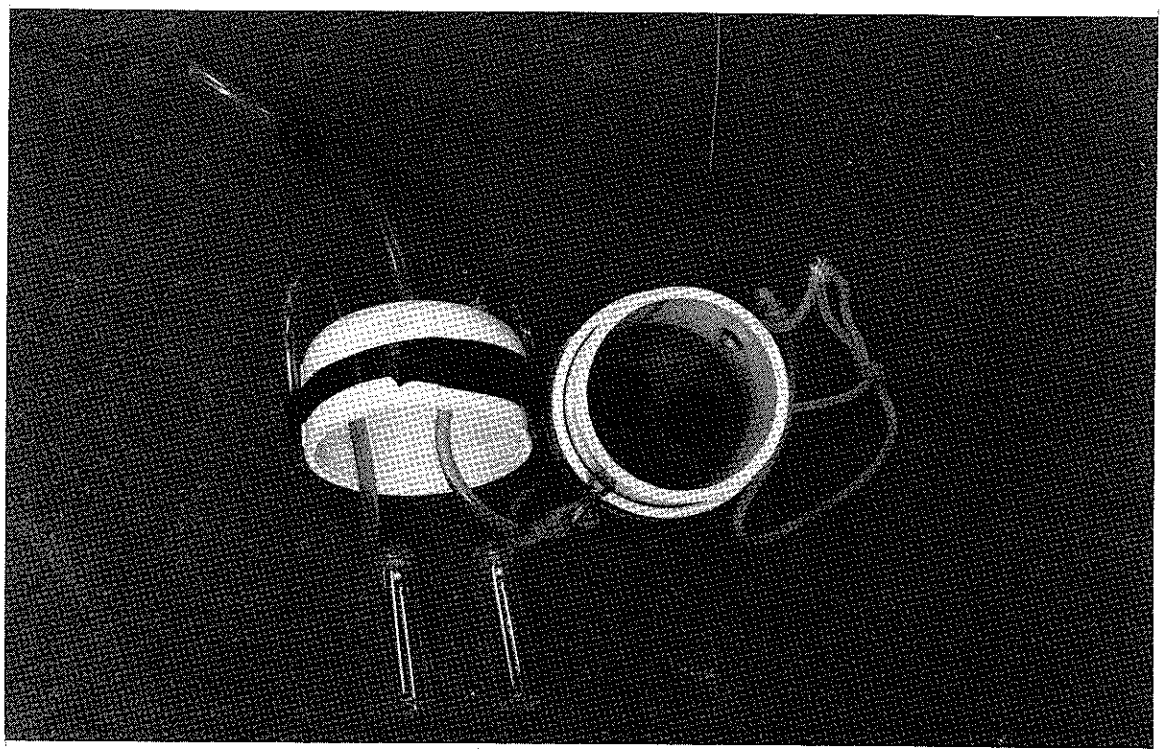

Photo 2. Water sampler

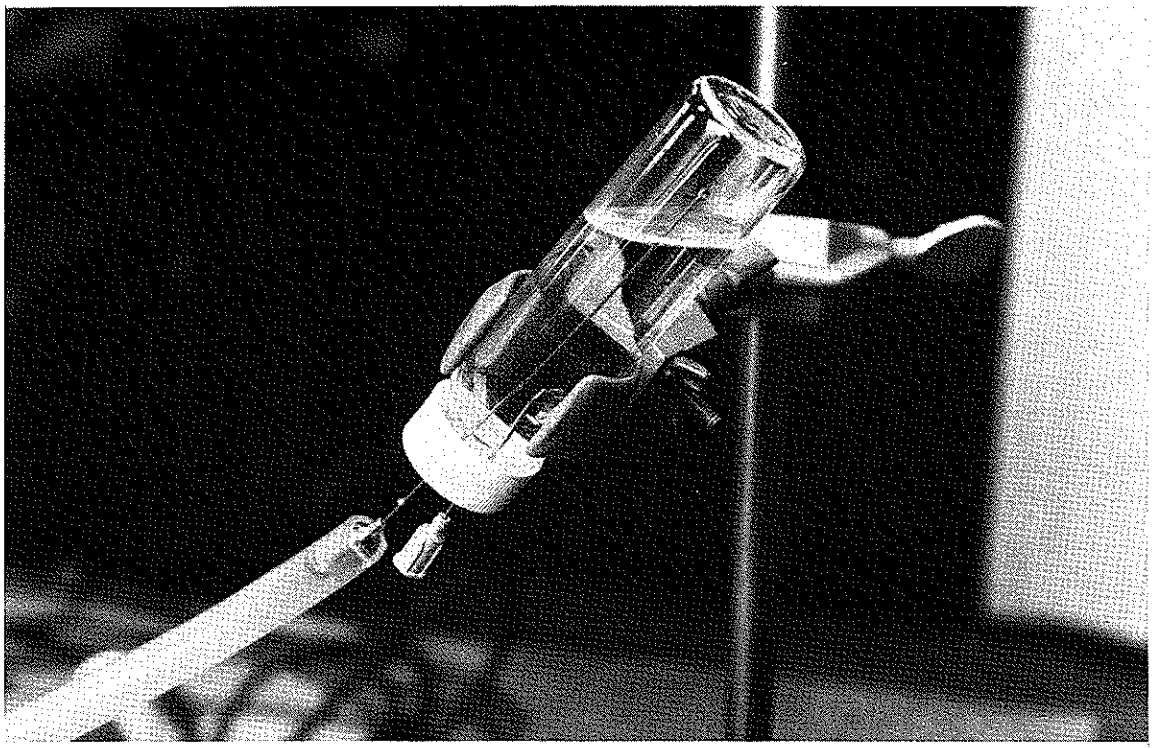

Photo 3. Creation of headspace in sample bottle

Appendix A
Air Entrainment Data

q_{air} measured at the Rum River Dam 2/17/90
q_{water} = 108 cfm/ft

Distance from plunge point ft	Run No. 1 q_{air} cfm/ft	Run No. 2 q_{air} cfm/ft
0.75	6.47	9.53
2.25	7.27	5.73
3.75	3.40	4.20
5.25	8.00	6.47
6.75	2.67	4.20
8.25	4.93	4.93
9.75	7.27	6.47
11.25	4.20	4.93
12.75	2.67	3.40
14.25	2.00	4.20
15.75	1.40	2.00
17.25	0.80	0.80
18.75	0	0
Total q_{air}	76.62	85.29

Appendix B
Description of Structures

Kost Dam

The Kost Dam is located on the Sunrise River in Chisago County, Minnesota. The dam consists of an ungated ogee spillway. A plan view and a profile view of the dam are shown in Figures B1 and B2, respectively.

Rum River Dam

The Rum River Dam is located on the Rum River, approximately 500 ft upstream of the Main Street Bridge in Anoka, MN. The structure consists of a 236-ft-long fixed weir, and a 20-ft-wide tainter gate. The tainter gate spillway is separated from the main river by a concrete pier. The plan view of the structure and the specific sampling locations are shown in Figure B3. The profile of the fixed weir is shown in Figure B4. The profile of the tainter gate and spillway is shown in Figure B5.

St. Cloud Dam

The St. Cloud Dam is located on the Mississippi River approximately 500-ft downstream of the 10th Street Bridge in St. Cloud, MN. The structure consists of a 500-ft-long fixed weir, and two tainter gates. The tainter gate spillway is separated from the main river by a concrete pier. The plan view of the structure and the sampling locations are shown in Figure B6. Only the tainter gate portion of the structure was investigated in this study. The profile of the tainter gate and spillway is shown in Figure B7.

Smithland Lock and Dam

The Smithland Lock and Dam is located on the Ohio River near Paducah, KY. A profile of the dam is shown in Figure B8.

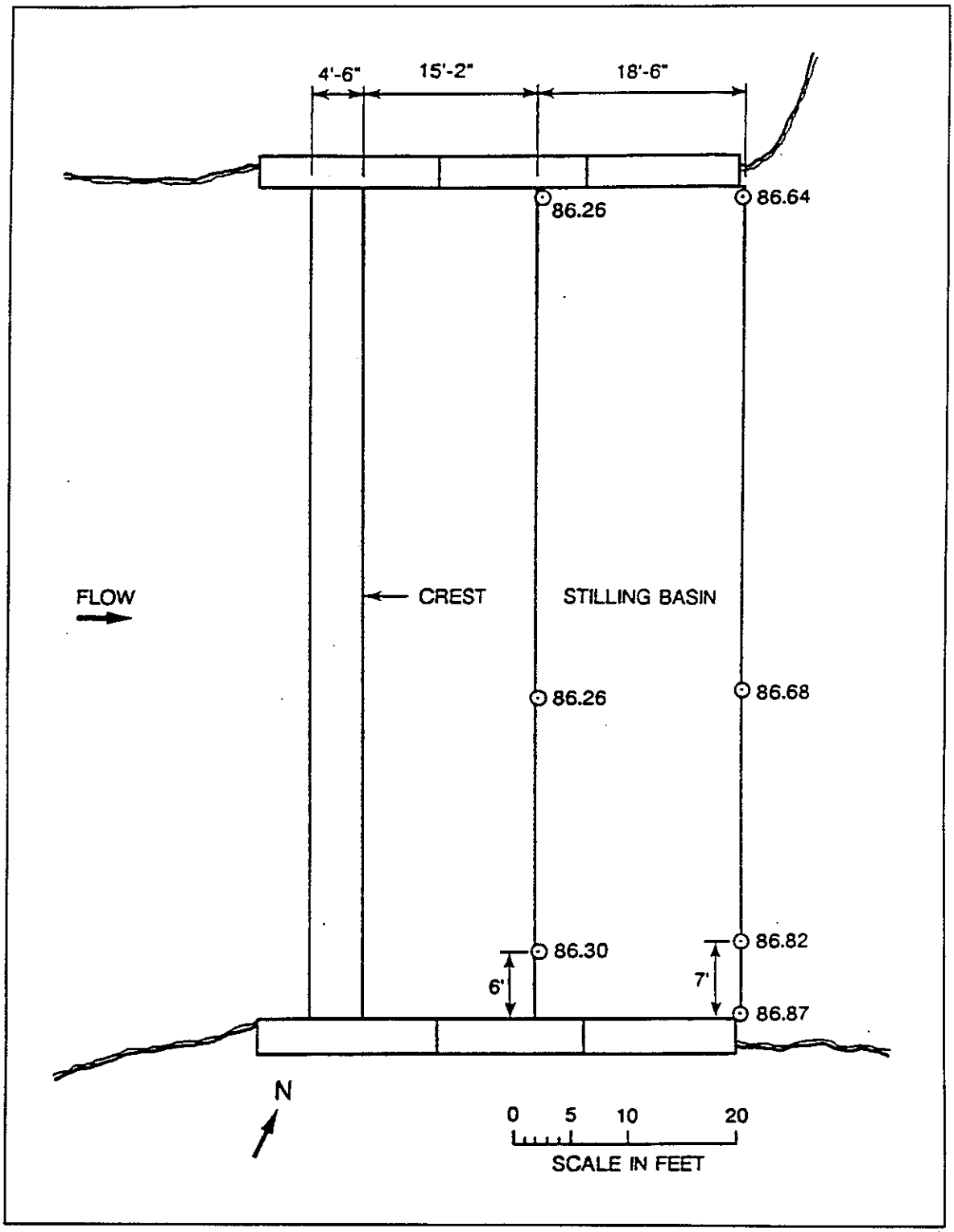

Figure B1. Plan view of Kost Dam

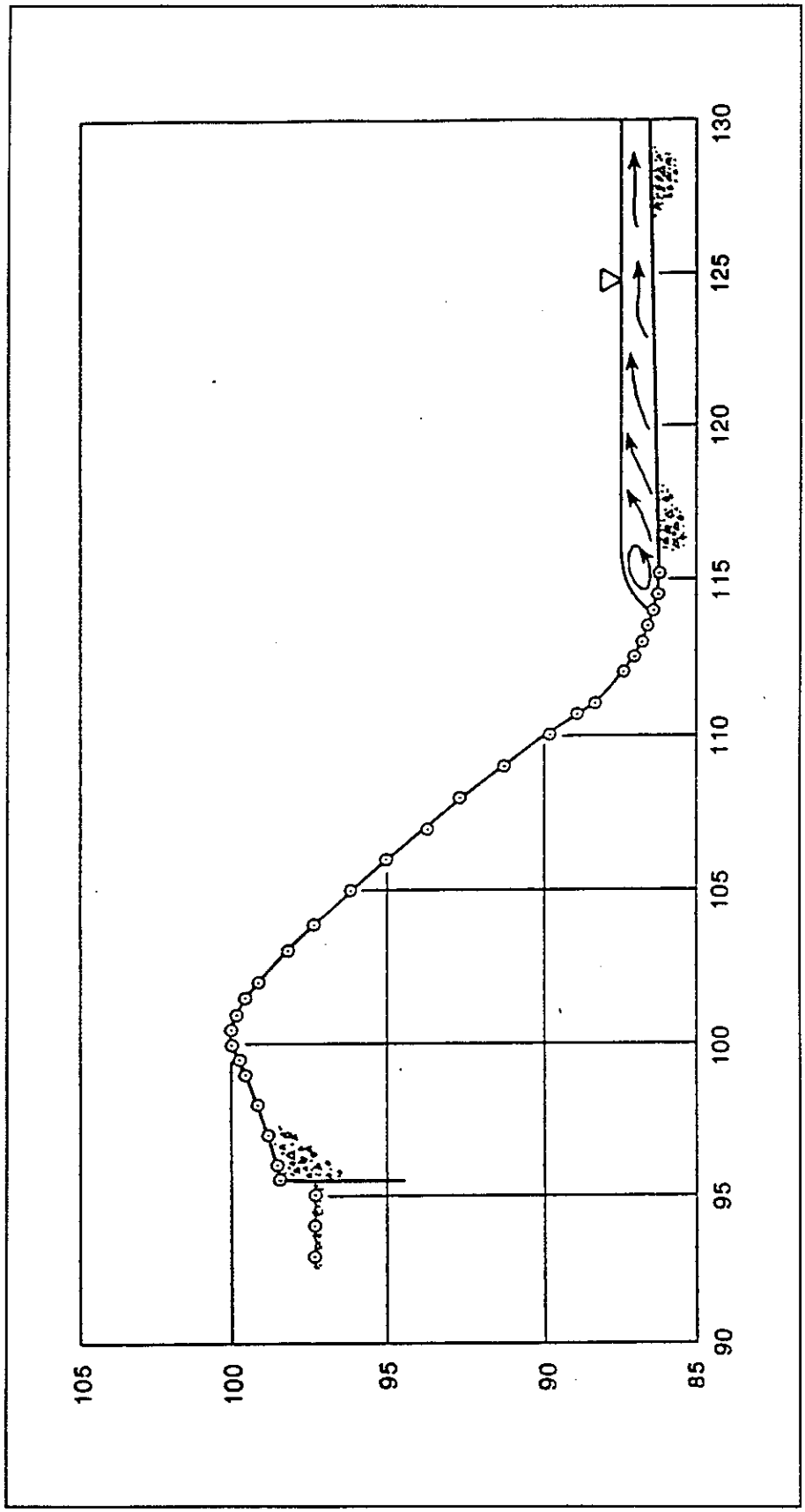

Figure B2. Profile view of Kost Dam

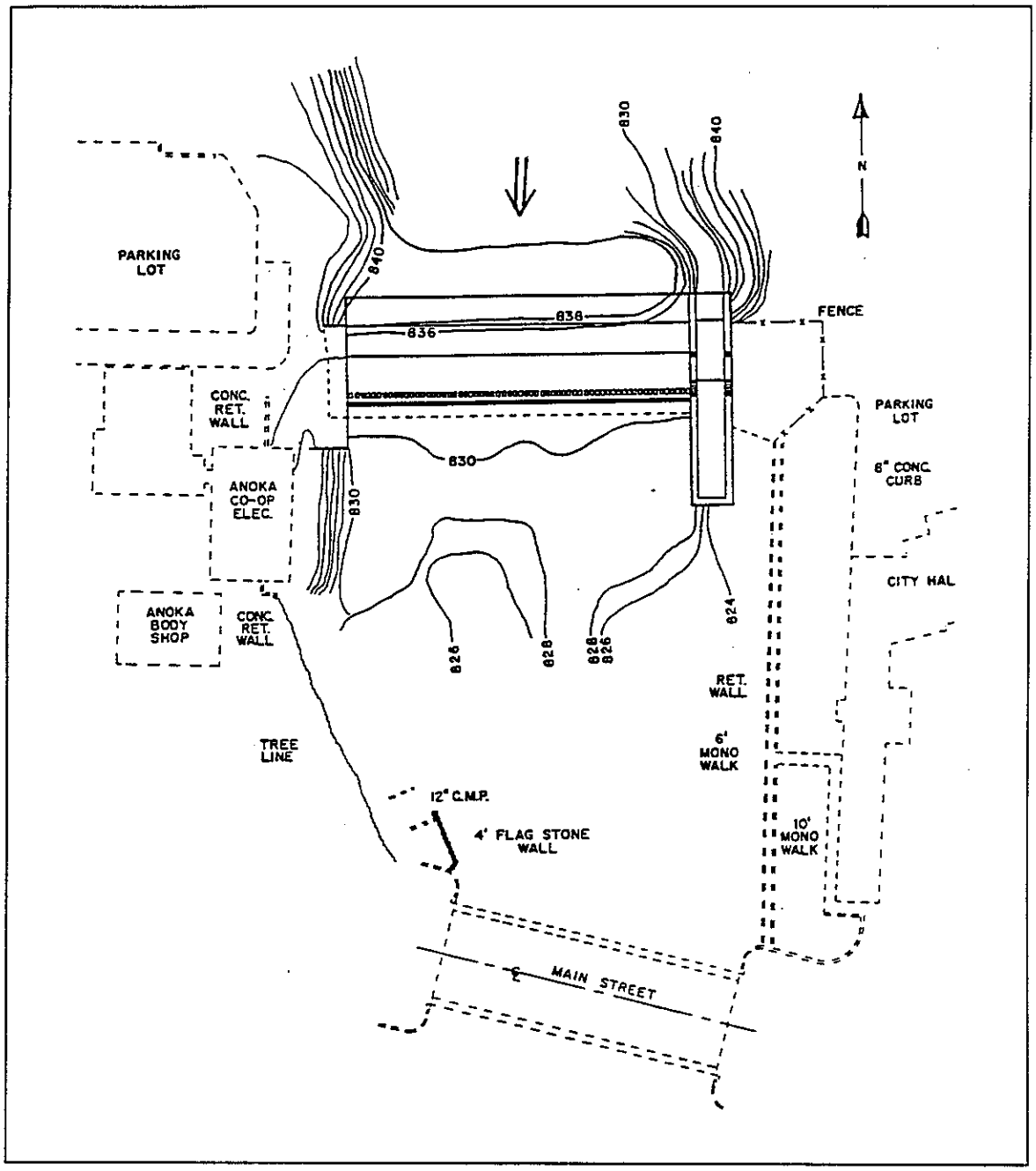

Figure B3. Plan view of Rum River Dam

Opekiska Lock and Dam

The Opekiska Lock and Dam is located on the Monogahelia River near Morgantown, WV. A profile of the dam is shown in Figure B9.

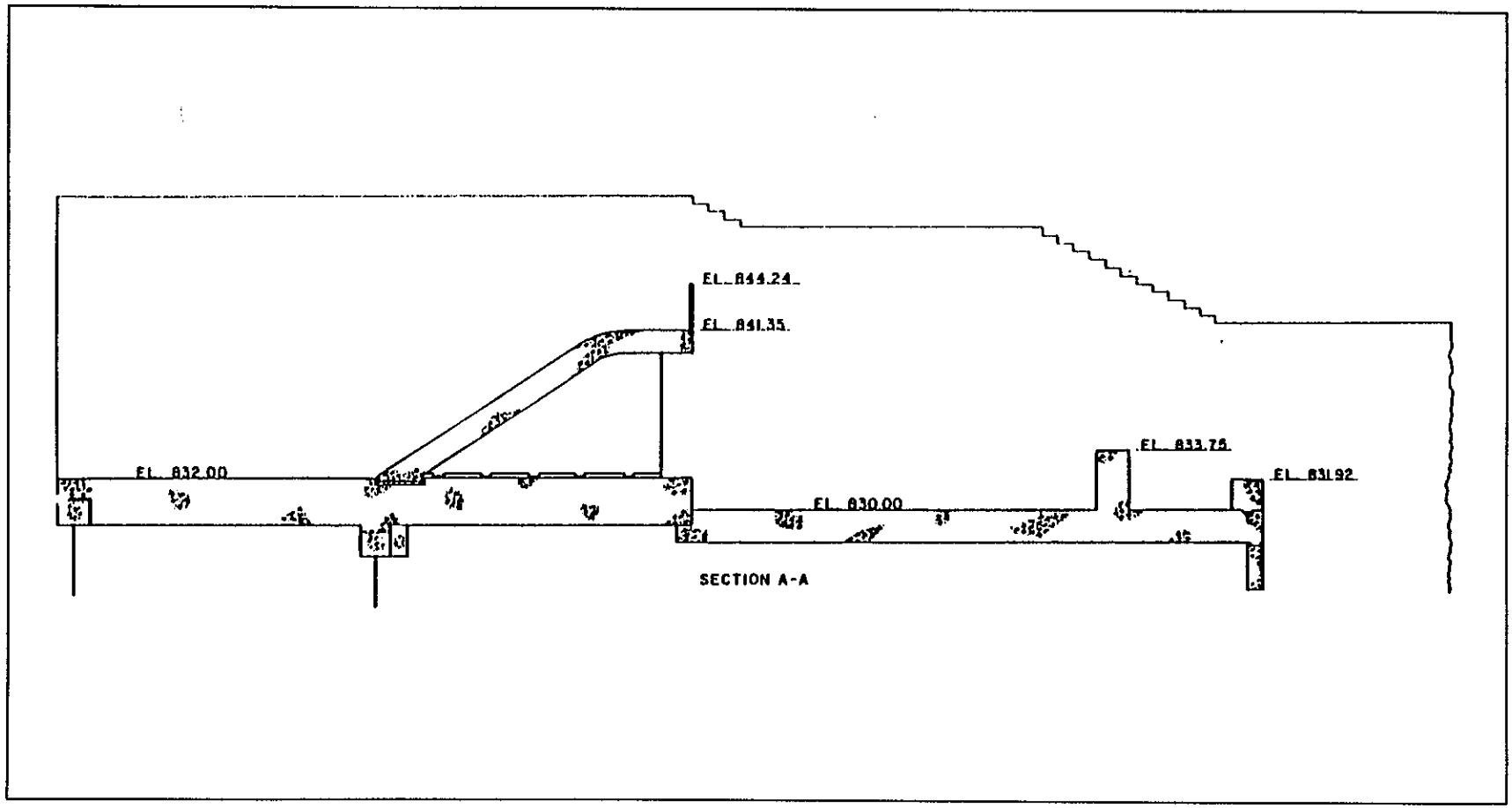

Figure B4. Profile of Rum River fixed weir

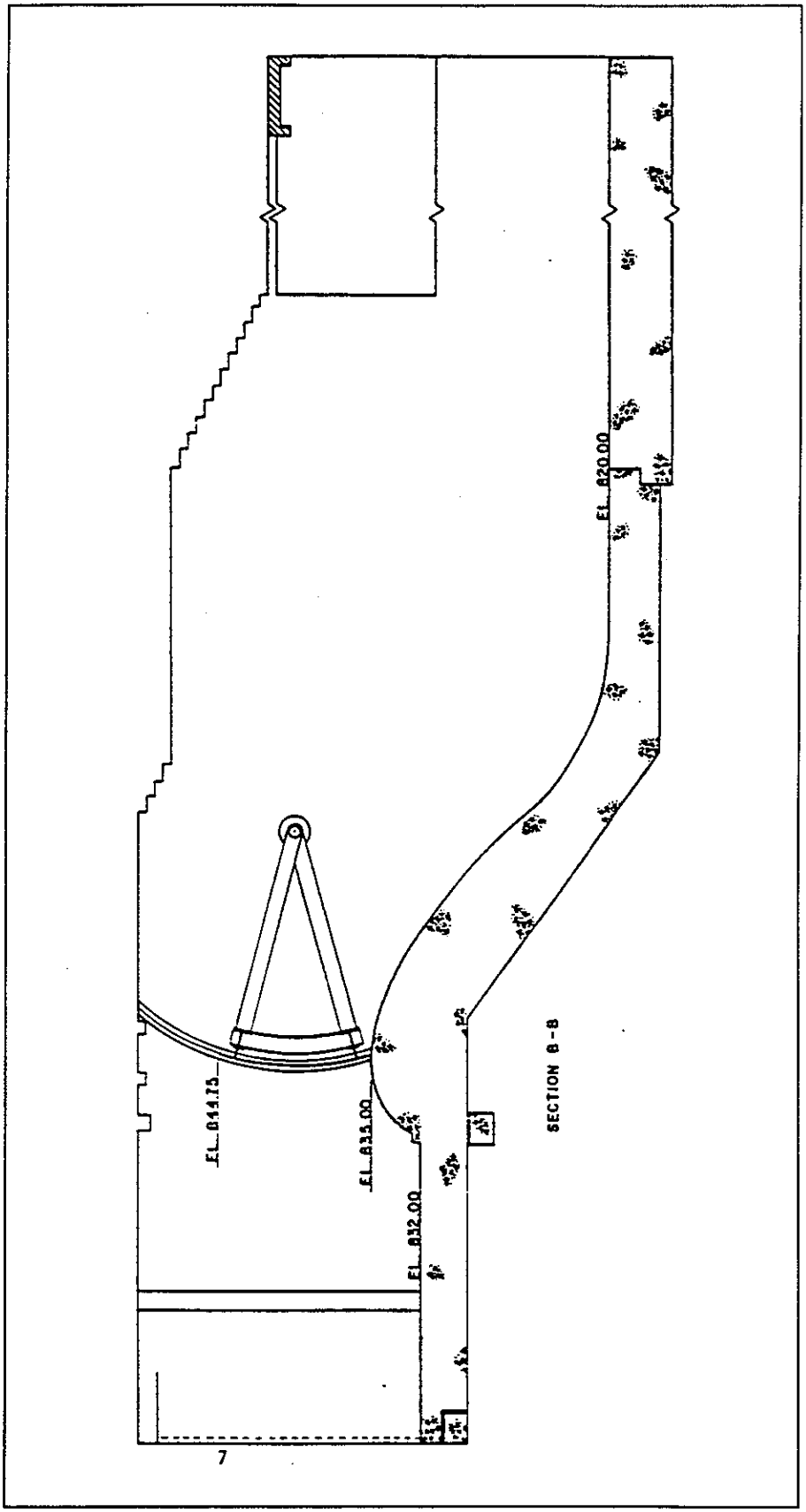

Figure B5. Profile of Rum River tainter gate

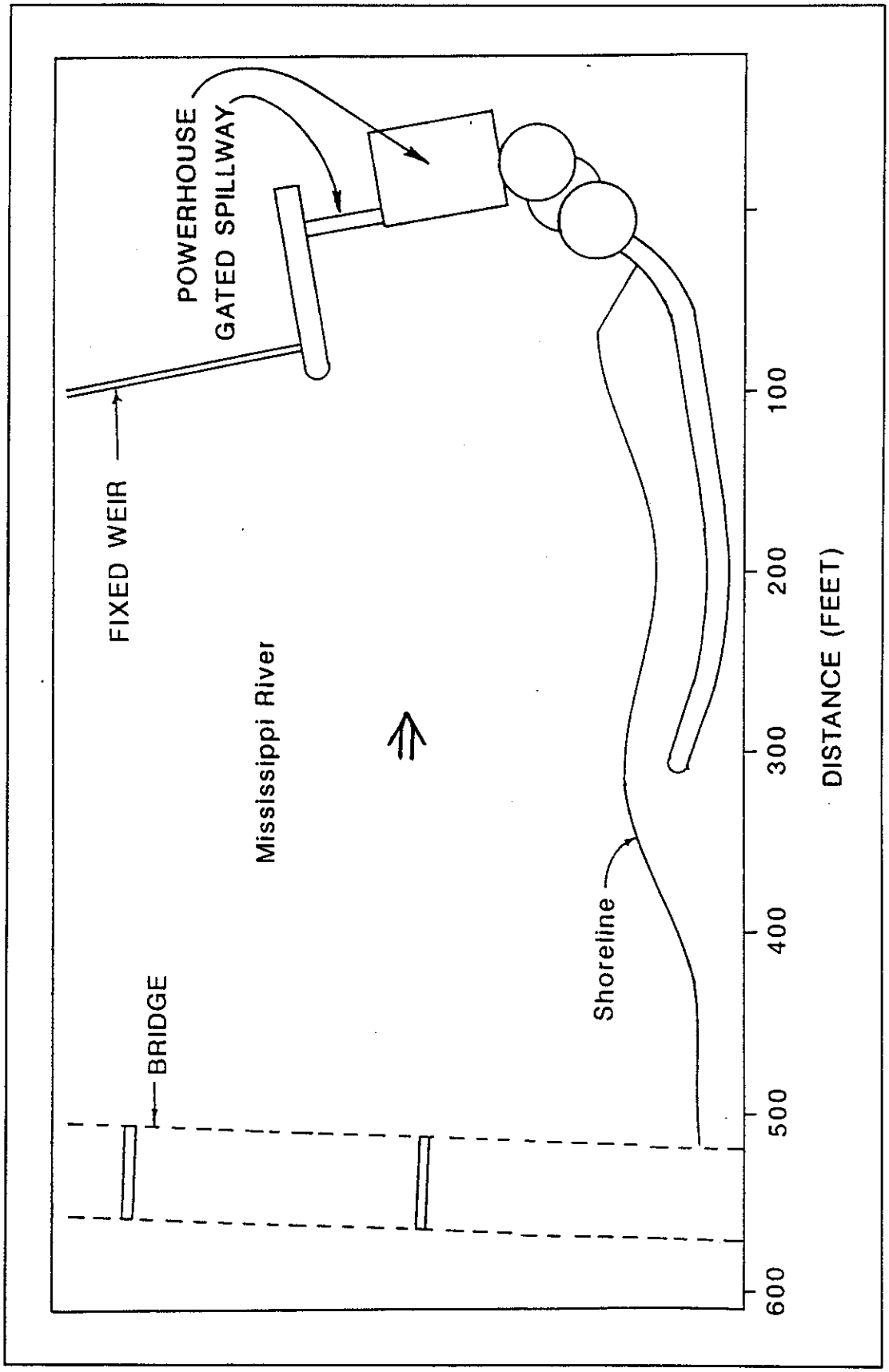

Figure B6. Plan view of St. Cloud Dam

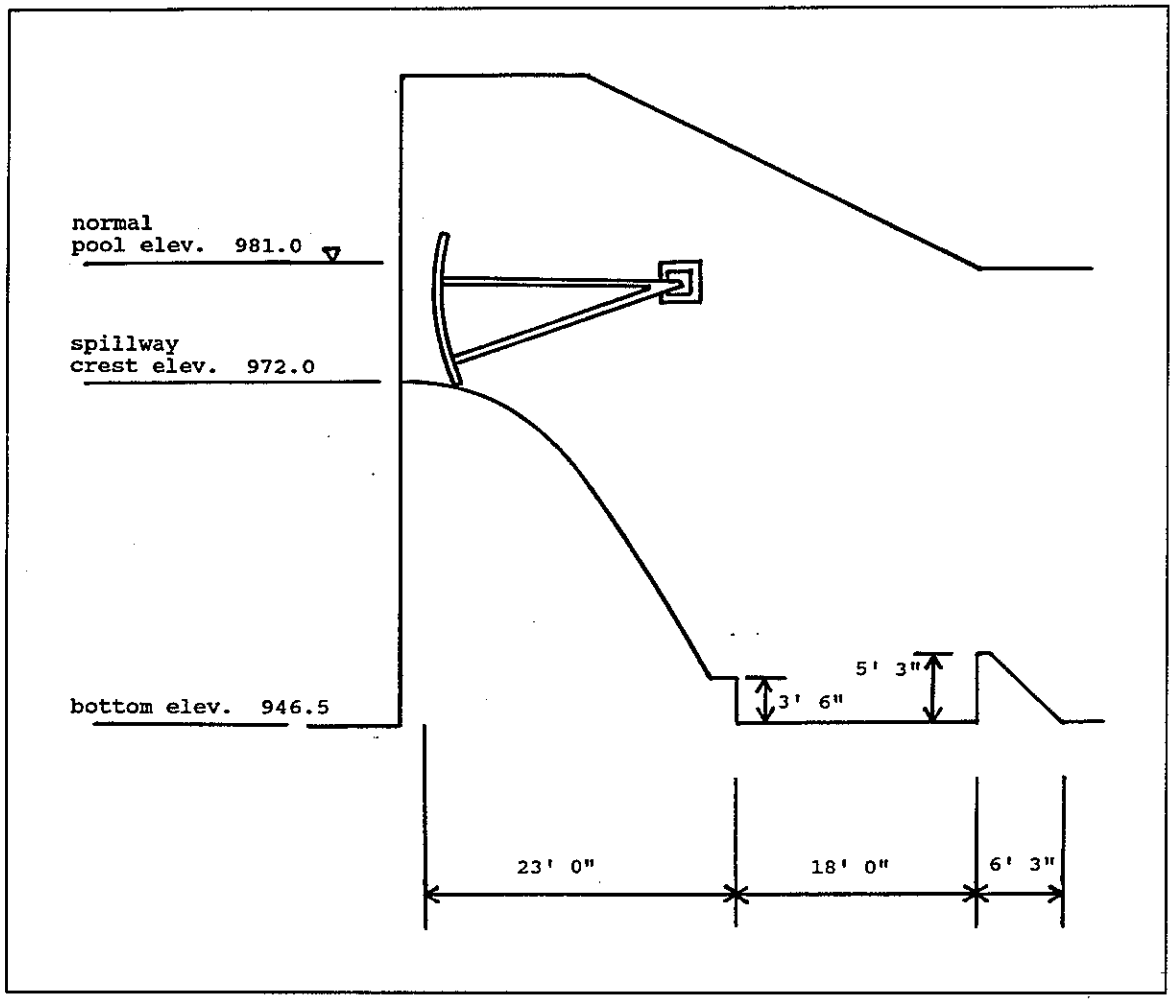

Figure B7. Profile view of St. Cloud Dam

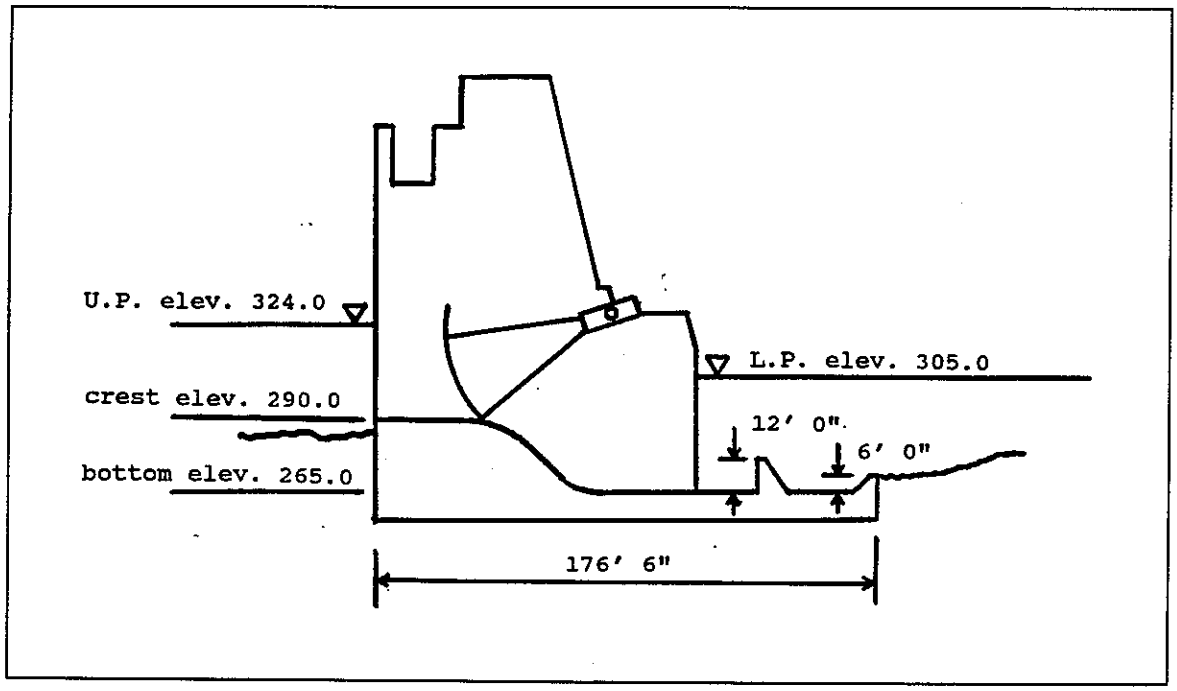

Figure B8. Profile view of Smithland Lock and Dam

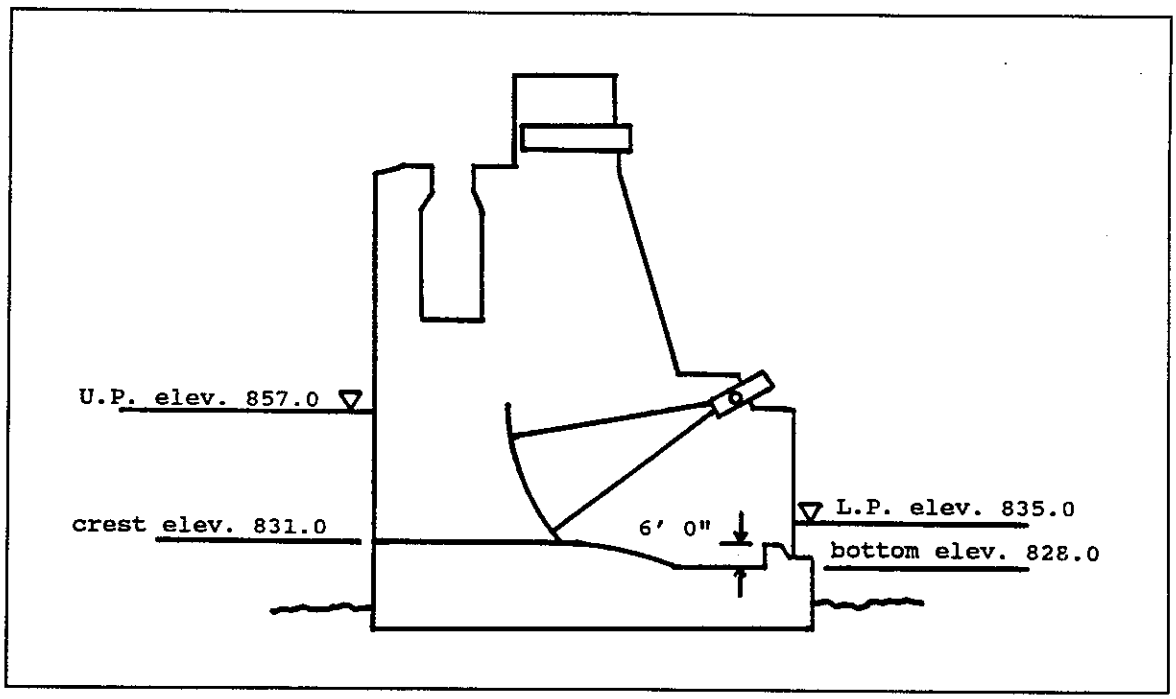

Figure B9. Profile view of Opekiska Lock and Dam

Appendix C
Notation

A	Air-water surface area
C	Concentration in water
C_a	Concentration in the air
C_b	Time averaged methane concentration in a bubble
C_d	Concentration downstream of the structure
C_m	Concentration of methane in a bubble as it is released to the atmosphere
C_{me}	Equilibrium concentration of methane in a bubble downstream of a structure
C_{N_2}	Dissolved nitrogen concentration
C_s	Saturation concentration
C_{se}	Effective saturation concentration
C_u	Concentration upstream of the structure
$comp$	Molar fraction of gas in the atmosphere
D	Diffusivity of the measured compound in the water
D_{eff}	Effective bubble depth
D_O	Diffusivity of oxygen in water
E	Gas transfer efficiency
E_m	Methane gas transfer efficiency
E_{iO}	Equivalent transfer efficiency of oxygen
F	Water surface flux of a volatile chemical per unit surface area
f_i	Indexing parameter for chemical and temperature
f_g	Indexing parameter for chemical
f_T	Indexing parameter for temperature
H	Henry's Law constant
K_L	Liquid film coefficient
K_p	Conversion constant from atmospheres to depth of water
M	Molecular weight of methane
P_{atm}	Barometric pressure
P_{H_2O}	Vapor pressure of water
P_{N_2}	Partial pressure of nitrogen
P_{O_2}	Partial pressure of oxygen
q_a	Specific air entrainment rate

q_w	Specific flow rate of water
R	Universal gas constant
t	Residence time
T	Water temperature
V	Control volume over which A and C are measured
V_a	Volume of headspace in a sample bottle
V_w	Volume of water in a sample bottle

REPORT DOCUMENTATION PAGE

Form Approved
OMB No. 0704-0188

Public reporting burden for this collection of information is estimated to average 1 hour per response, including the time for reviewing instructions, searching existing data sources, gathering and maintaining the data needed, and completing and reviewing the collection of information. Send comments regarding this burden estimate or any other aspect of this collection of information, including suggestions for reducing this burden, to Washington Headquarters Services, Directorate for Information Operations and Reports, 1215 Jefferson Davis Highway, Suite 1204, Arlington, VA 22202-4302, and to the Office of Management and Budget, Paperwork Reduction Project (0704-0188), Washington, DC 20503.

1. AGENCY USE ONLY *(Leave blank)*

2. REPORT DATE
September 1995

3. REPORT TYPE AND DATES COVERED
Final report

4. TITLE AND SUBTITLE
Methane Sampling Technique and the Measurement of Plunge Pool Impact on Gas Transfer Rates at Low-Head Hydraulic Structures

5. FUNDING NUMBERS

6. AUTHOR(S)
David E. Hibbs, John S. Gulliver, John P. McDonald

7. PERFORMING ORGANIZATION NAME(S) AND ADDRESS(ES)
St. Anthony Falls Hydraulic Laboratory, Department of Civil and Mineral Engineering, University of Minnesota, Mineapolis, MN 55455;
Zenk Read Trygstad and Associates, Inc., Albert Lea, MN 56007

8. PERFORMING ORGANIZATION REPORT NUMBER

9. SPONSORING/MONITORING AGENCY NAME(S) AND ADDRESS(ES)
U.S. Army Corps of Engineers, Washington, DC 20314-1000;
U.S. Army Engineer Waterways Experiment Station, 3909 Halls Ferry Road, Vicksburg, MS 39180-6199

10. SPONSORING/MONITORING AGENCY REPORT NUMBER
Miscellaneous Paper W-95-2

11. SUPPLEMENTARY NOTES
Available from National Technical Information Service, 5285 Port Royal Road, Springfield, VA 22161.

12a. DISTRIBUTION/AVAILABILITY STATEMENT
Approved for public release; distribution is unlimited.

12b. DISTRIBUTION CODE

13. ABSTRACT *(Maximum 200 words)*

In situ dissolved methane gas was used as a tracer for estimating the gas transfer rates of flow over low-head hydraulic structures. The methane measurement provided a means to assess the effects of the plunging flow in the structure stilling basin. Simultaneous oxygen-methane transfer measurements and nitrogen-methane measurements were used to develop the concept of an "effective depth," which is the mean depth to which entrained air bubbles are transported in the stilling basin. Generally, as discharge increased, the mean depth increased probably as a consequence of the increase in momentum. Effective depths computed with oxygen-methane measurements were very similar to effective depths computed with oxygen-nitrogen measurements, thus verifying the concept of effective depth. Additional measurements should be performed at other structures to relate the effective depth to parameters of the spillway jet and stilling basin.

14. SUBJECT TERMS
Gas transfer
Hydraulic structures
In situ methane
Plunge pools
Reaeration
Stilling basin
Tracer gas

15. NUMBER OF PAGES
69

16. PRICE CODE

17. SECURITY CLASSIFICATION OF REPORT
UNCLASSIFIED

18. SECURITY CLASSIFICATION OF THIS PAGE
UNCLASSIFIED

19. SECURITY CLASSIFICATION OF ABSTRACT

20. LIMITATION OF ABSTRACT